721

ISSN 0868-4081
0868-4138

TALLINNA TEHNIKAÜLIKOOLI

TOIMETISED

ТРУДЫ ТАЛЛИННСКОГО ТЕХНИЧЕСКОГО УНИВЕРСИТЕТА

TRANSACTIONS OF TALLINN TECHNICAL UNIVERSITY

ENGINEERING STRUCTURES
AND STRUCTURAL MECHANICS
XXIX

TALLINN 1990

№ 721

TALLINNA TEHNIKAÜLIKOOLI TOIMETISED

ТРУДЫ ТАЛЛИННСКОГО ТЕХНИЧЕСКОГО УНИВЕРСИТЕТА

СТРОИТЕЛЬНЫЕ КОНСТРУКЦИИ И СТРОИТЕЛЬНАЯ МЕХАНИКА XXIX

УДК 624.074.4:530.182

Фракталы в инженерном деле. Энгельбрехт Ю.К. Труды Таллиннского технического университета 1991. № 721, с. 3-11.

В статье приведены основные понятия теории фракталей, которые могли бы быть применены в проектировании железобетонных конструкций и оболочек. Одна из основных проблем – это моделирование трещин в элементах, работающих на растяжение. Коротко описана теория, позволяющая на основе дискретизации моделировать рост трещин с определенной условностью. Приведен ряд проблем, решение которых целесообразно при помощи теории фракталей.

Рисунков – 3, библ. наименований – 13.

УДК 624.074

Висячие покрытия в качестве акустических экранов для певческих эстрад в Эстонии. Кульбах В.Р. – Труды Таллиннского технического университета 1991. № 721, с. 12-20.

Акустические экраны Таллиннской певческой эстрады, возведенной в 1960 году, и Тартуской эстрады, строящейся с 1989 года, представляют собой различные седловидные висячие покрытия. Контур Таллиннского экрана состоит из двух плоских арок, опертых на массивные контрфарсы; контур Тартуского экрана имеет форму замкнутой пространственной кривой эллиптической формы и опирается на три плоские вертикальные диафрагмы, которые не препятствуют деформациям контура в горизонтальных направлениях. Значительные различия имеются также в конструирова-

нии сети вант и в соединениях вант с контуром. Особенностью Тартуского экрана является значительно меньшее значение усилий предварительного напряжения по сравнению с Таллиннском экраном. Этому способствуют действия нагрузок, приложенных к сети и к контуру, а также увеличиваются усилия как в несущих, так и в стягивающих вантах.

В статье приводятся основы для определения усилий и перемещений обоих экранов, исходя соответственно из дискретной или континуальной расчетной схемы.

Рисунков - 2, библ. наименований - 2.

УДК 624.074

Статическое нагружение модели акустического экрана. Кульбах В.Р., Паане П.А. - Труды Таллиннского технического университета. 1991. № 721, с. 21-31.

Представлены результаты экспериментального исследования модели седловидного покрытия с контуром в виде эллипса и вантовой сетью из круглой стали. Модель изготовлена в масштабе 1:10, полуоси эллипса 2,7 и 2,1 м. Покрытие опирается на три парные опоры, которые не препятствуют горизонтальным перемещениям контура. Передняя часть контура свободно перемещается в вертикальном направлении. Рассматривается влияние разных нагрузок, приложенных в узлах сети, а также нагрузок, распределенных по длине контура. Действие собственного веса контура может быть использовано для преднапряжения вантовой сети. В статье приводятся графики, иллюстрирующие распределение усилий и перемещения вантовой сети.

Таблиц - 1, рисунков - 13, библ. наименований - 2.

УДК 624.074

Определение динамических характеристик седловидного висячего покрытия. Нийгер К.П., Тальвик И.Р. - Труды Таллиннского технического университета. 1991. № 721, с. 32-38.

Представлены результаты динамического испытания модели седловидного покрытия с контуром в виде эллипса и вантовой сетью из круглой стали. Модель изготовлена в

масштабе I:I0, полуоси эллипса 2,7 и 2,I м. Покрытие опирается на три парные плоскостные опоры, которые не препятствуют горизонтальным перемещениям контура. Передняя часть контура может свободно перемещаться также в вертикальном направлении. Настил выполнен в виде трехслойной деревянной оболочки. Рассматривается влияние разных нагрузок, распределенных по длине контура, а также в узлах сети на собственные частоты конструкции при наличии настила и без него. Численно определенные собственные частоты для конструкции с настилом близки к экспериментальным.

Рисунков - 5, библ. наименований - 2.

УДК 624.074.4.0I2.45.00I.5(474.2)

Исследование принципов работы оболочек двоякой кривизны при помощи моделей. Тярно Ю.А. - Труды Таллиннского технического университета. 1991. № 721, с. 39-49.

С 1955 по 1975 годы по инициативе и под руководством члена Эстонской Академии наук профессора Х. Лаула представителями его школы был проведен ряд экспериментально-теоретических исследований цилиндрических железобетонных оболочек. В результате этой обширной работы стало возможным сделать обобщения для поведения оболочек с трещинами, изготовленных из имеющегося материала (армоцемент,железобетон).В последующие годы для уточнения и дополнительного обобщения проделанной работы исследовалось влияние на оболочки двоякой кривизны различных кривизн как упругой стадии, так и в стадии возникновения трещин для широкого диапазона геометрических параметров и нагрузок [I, 2].

В настоящей работе рассматриваются оболочки с положительной, нулевой и отрицательной кривизной, средней длины с различными жесткостями краевых элементов и условиями опирания. Влияние продольных, поперечных и наклонных трещин, также шарниров на распределение внутренних сил исследовалось на упругой модели с искусственными трещинами.

Исследованное в работе применение предварительно напряженных элементов позволяет изменить величины и распределение внутренних сил в желательном для конструктора направлении. Для систематизирования внутренних сил используются обобщенные схемы и безразмерные параметры.

Рисунков - 2, библ. наименований - 25.

УДК 624.074

Обеспечение прочности стальных цилиндрических аппаратов колонного типа при монтаже. Гордон Э.Я. Труды Таллиннского технического университета. 1991. № 721, с. 50-59.

Особое место при сооружении объектов нефтяной и химической промышленности занимает монтаж аппаратов колонного типа. Подъемная масса таких аппаратов может достигать 1000 т при высоте до 100 м.

В процессе подъема стенка цидиндрического корпуса аппарата в местах присоединения строповых устройств и монтажных приспособлений воспринимает значительные локальные нагрузки в виде изгибающих моментов, радиальных и тангенциальных сил.

В связи со сложными условиями работы реактора Институтом Гипронефтеспецмонтаж совместно с Таллиннским техническим университетом были проведены экспериментальнс-теоретические исследования по определению напряженно-деформированного состояния цилиндрических оболочек от монтажных нагрузок. Для теоретического исследования поставленной задачи использовали метод конечных элементов.

Теоретические результаты работы показали, что напряженно-деформированное состояние цилиндрической оболочки носит ярко выраженный локальный характер.

На основании проведенных экспериментально-теоретических исследований и опыта практического выполнения монтажных работ была разработана методика расчета прочности корпуса колонного аппарата в процессе монтажа.

Рисунков - 3, библ. наименований - 6.

ALUSTATUD 1937

TALLINNA TEHNIKAÜLIKOOLI TOIMETISED

TRANSACTIONS OF TALLINN TECHNICAL UNIVERSITY

ТРУДЫ ТАЛЛИННСКОГО ТЕХНИЧЕСКОГО УНИВЕРСИТЕТА

UDC 624.01/04

ENGINEERING STRUCTURES
AND STRUCTURAL MECHANICS
XXIX

TALLINN 1990

Contents

Editor V. Jaaniso

TTÜ, 1991, 300, 257
Rbl. 1.50

No 721

TALLINNA TEHNIKAÜLIKOOLI TOIMETISED
TRANSACTIONS OF TALLINN TECHNICAL UNIVERSITY

UDC 624.074.4:530.182

J. Engelbrecht

FRACTALS IN ENGINEERING

"What do you know about this business?" the King said to Alice. "Nothing whatever," said Alice.

Lewis Carrol

Allegro moderate

The idea to write a paper on fractals in engineering came to the author in Cambridge when he was reading the special number of Physica D (1989, vol. 38, Nos 1-3) dedicated to B.B. Mandelbrot. It was anno 1989 and the author was already aware of the forthcoming anniversary volume dedicated to Heinrich Laul. The preliminary plan was to describe some remarkable new theories in connection with the long outstanding research work carried out by him. However, his active role in developing the theory of concrete shells and his consulting practice during the last half of a century have set some natural limitations to the preliminary idea. Consequently, in this paper only one branch of engineering - mechanics of concrete structures - is discussed. The point of view taken by the author differs considerably from the common engineering practice. The aim of this paper is to point out some fascinating new problems for concrete structures on the basis of the theory of fractals. This is done despite the motto given above.

The word "fractal" is coined by B.B. Mandelbrot in 1975 in order to describe "rough but selfsimilar" objects

[1]. As it is now widely known, everything has started from the famous mapping $z \rightarrow z^2 + c$ in the complex plane, investigated by B.B. Mandelbrot, which gave rise to the famous "ginger-bread man" or Mandelbrot set [1, 2]. However, J. Hubbard says that he has investigated this mapping some years earlier but as it sometimes happens in science, no traces of this research are known except the author's statement [3].

What are fractals? F. Hundertwasser has said that "the straight line leads to the downfall of the mankind" [2]. This "slight exaggeration" has deep roots. We are all accustomed to school geometry starting, for example, from Galileo Galilei and his famous statement: "It (i.e. the Universe) is written in the language of mathematics and its characters are triangles, circles and other geometric figures, without which it is humanly impossible to understand a single word of it..." (taken from [2]). Only nowadays, about 350 years later, we know that "clouds are not spheres, mountains are not cones, coastlines are not circles, and bark is not smooth, nor does lightning travel in a straight line" [40, 93]. This is exactly what B. Mandelbrot meant using the word "fractal", which really gives new insight in describing coastlines and rivers, islands and mountains, grains in rock, metal and composites, clouds and turbulent flows, growth of plants and cells, particle trajectories and clusters, etc.

However, a complete definition of fractals is still not known [5]. One could use an intuitive definition [6]:

A fractal is a shape made of parts similar to the whole in some way.

A tentative, more strict definition reads [6]: A fractal is a set for which the Hausdorff-Besicovitch dimension strictly exceeds the topological dimension.

This definition requires other definitions for terms used in it. The topological dimension D_T is meant here in its usual sense: the set of points that make up a line in ordinary Eucleidean space has $D_T = 1$, the set of points that form a surface in the same space has $D_T = 2$, a sphere has $D_T = 3$, etc. Topological dimension D_T is

always an integer. The Hausdorff-Besicovitch dimension D_H measures properties of sets of points forming a "rough" line, surface, space, etc. in the limit of a vanishing diameter or size δ of the test function used to cover the set. It may be surprising but D_H needs not to be an integer. Still, for a line $D_T = D_H = 1$, for a plane $D_T = D_H = 2$. But for a coast-line or for a cluster the result is that D_H is a noninteger. For example, in Fig. 1 the two-scale Cantor set with nonidentical segments is shown ($l_1 = 1/4$; $l_2 = 2/5$) in the unit interval [0, 1]. Here we get $D_H = 0{,}6110$, i.e. this set is something between a line and an empty set of points [6]. Sometimes D_H is called fractal dimension. The reader is referred to monographs in this field in order to obtain more examples [2, 4, 6, 7]. It is obvious that the possibilities of fractal geometry are much wider than those of Eucleidean geometry and many natural objects compiled by "broken" lines, surfaces or spaces could be effectively described by fractals.

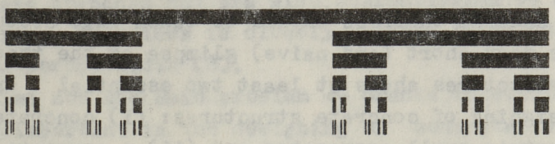

Fig. 1. Five first generations of the two-scale Cantor set with $l_1 = 1/4$ and $l_2 = 2/5$ [6].

Andante

H. Laul knows a lot about concrete and concrete structures. In order to put concrete and fractals together, we also need some description of concrete as a material. In a concise form the following description may be given [8] : concrete is "a versatile engineering material consisting of a hydraulic cementing substance, aggregate, water, and often controlled amounts of entrained air. Strength is developed in the hydration reaction between the cement and water. The products, mainly calcium silicates, calcium aluminate, and calcium hydroxide, are relatively insoluble and bind the aggregate in a hardened matrix". As to the aggregate, beside natural sands and gravels, crushed limestone is widely used in Estonia.

The most important feature of concrete is that it works much better under the compressive stresses rather than tension. Usually the structural elements under bending and shear induce tensile stresses and they are designed under the assumption that tensile stresses have cracked the concrete and the steel reinforcing carries all the tension.

The cracks are very important indeed in describing the behaviour of concrete structures. Particularly, in concrete shells some special problems are met which can be summed up in the following way [9]: the reinforcement is sometimes not used in shells either for some reasons of economy (cracks in cylindrical shells are not considered to be essential in case of stringer-type border elements) or for structural purposes (the curved part of a shell is designed not to accept torsional forces). It is also known [9] that in the first case the usual shell theory can sometimes still be applied but in the second case the pattern of internal forces is completely different and therefore special theories should be taken into account.

This very short (and naive) glimpse at the theory of concrete structures shows at least two essential points in the designing of concrete structures: (i) concrete is made of certain small aggregates and (ii) a concrete structure usually has cracks. Even the compressed description of fractals given in the previous section leads immediately to a natural question — is the notion of fractals of some use in describing the behaviour of concrete structures? Below, some ideas for answering this question are outlined.

Scherzo

Let us try first to characterize concrete as inhomogeneous material. It is useful to point out that in contemporary understanding inhomogeneous materials can be divided into two groups [10]:

- energetic elasticity group, i.e. materials the elementary grains of which are very large;
- entropic elasticity group, i.e. materials consisting of very small building blocks.

Concrete, sandstone, etc. belong to the first group, and composite materials, rubbers, etc. – to the second group. For the first group of materials entropy remains unchanged during the deformation while for the second group, entropy is changed due to distortion which leads to changes in energy. Such an understanding may be useful in constructing the constitutive equations.

Establishing such a general property, we come to an important problem of how stress is transmitted in aggregated media. Using the notion of fractals, it is clear that concrete is a fractal-like material: the aggregates are stuck together by a cementing substance forming a 3-dimensional cluster. A natural question immediately arises: can concrete be characterized by a fractal dimension which is actually an additional quantitative measure? The answer to this question (not known to the author) would help to understand how concrete sustains stress and how that stress is transmitted. According to Edwards and Oakeshott [11], stress in fractal-like materials is transmitted in one-dimensional paths which are branched and are also characterized by a fractal dimension. This idea is closely related to percolation problems in porous media [6].

And now the main problem — cracks in concrete which are so important in the designing of concrete structures, particularly of concrete shells [9]. It can be agreed without any doubt that cracks are of fractal nature. Nevertheless, not very much is known about the real mechanisms of the growing of the cracks. One possible mechanism is based on discrete elementary beams, used by H.J. Hermann [12]. Further on, his results concerning the growth of an existing single crack are briefly referred to.

In this problem, three main equations occur. First, the medium is described by the Lamé equation

$$(\lambda + \mu)\,\nabla\,(\nabla\cdot\vec{u}) + \mu\nabla^2\vec{u} = 0 \qquad (1)$$

where λ, μ are the Lamé coefficients and $\vec{u}$ is the displacement vector. For an existing crack, the stress normal to the surface of the crack is zero and the crack will grow in the direction perpendicular to the surface at the point

where the strain parallel to the surface is the largest. The growth depends on the elastic energy, or, actually, how the elastic energy is transported away from the growing tip. The normal growth velocity $\vec{v}_n$ is given as

$$\vec{v}_n \sim [(\sigma_{\parallel} \vec{u}_{\parallel})^2 + q\sigma_{\parallel}^2 \vec{u}_{\perp}]^{\eta} \qquad (2)$$

where q and η are material-dependent parameters and other notations are obvious. If $\eta = 1$, then the von Mises yielding criterion is taken as a basic one. As for q, it emphasizes the affinity of the breaking process to the bending mode as compared to cleavage (transverse action). The process is discretized by using elementary beams which physically means introducing anisotropy and a cutoff at small length scales. The breaking of a beam is determined by a quantity p governed by the third equation

$$p = [f^2 + q \max(|m_1|, |m_2|)]^{\eta} \qquad (3)$$

where f is the fraction force and m_1, m_2 are the moments acting at the two ends of the beam. Three criteria involving the value of p, are used in [12]. Criterion I describes ideally brittle and fast rupture; criterion II accounts for slower cracks which could happen during fast stress corrosion effects (actually a short time memory is taken into account); criterion III is applied for slow stress corrosion effects (static fatigue). The criteria are related to each other by combining the value of f in (3).

Applying the criterion I, the cracks are not fractal-like [12]. This could be in some sense compared with the fracture of a glass-like material with long smooth cracks. The fractal dimension of a crack obtained by the criterion III is higher than that obtained by the criterion II. This is shown in Fig. 2 taken from [12]. Are these criteria applicable for real situations? Theoretical and experimental cracks are compared in the case of the alloy Ti - 11.5 Mo - 6 Zn - 4.5 Sn (not for concrete!) [12]. These results are shown in Fig. 3 and a "vague" similarity can really be seen. The fractal dimensions for these cracks are not given but some estimates are known for fracture surfaces of metals.

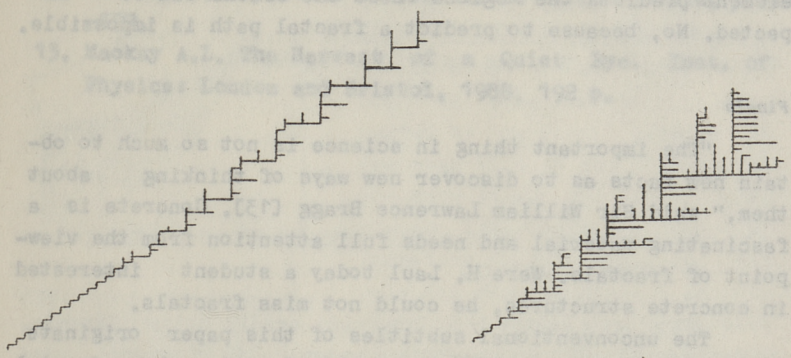

Fig. 2. Theoretical cracks in discrete system under external shear using criterion II (a) and criterion III (b) [12].

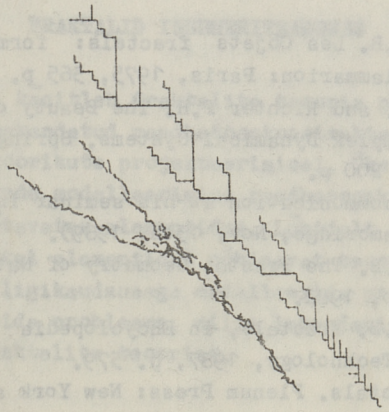

Fig. 3. Theoretical (criterion II) and experimental cracks for an alloy (details given in [12]).

According to [6], $D_H \approx 2.1 \ldots 2.28$. For cracks in concrete, no estimates are known to the author.

There are many questions not answered yet. For example: given the fractal dimension of a crack, what traction can be applied to it? Or another question: given the crack and its measured fractal dimension (for measuring technique see [6, 7]), can the nature of the traction that has caused the crack be determined? And the most fascinating question: can cracks be predictable? Here probably the answer is yes and no. Yes, because the stress distribution in a structural

element predicts the regions where the cracks can be expected. No, because to predict a fractal path is impossible.

Finale

"The important thing in science is not so much to obtain new facts as to discover new ways of thinking about them," said Sir William Lawrence Bragg [13]. Concrete is a fascinating material and needs full attention from the viewpoint of fractals. Were H. Laul today a student interested in concrete structures, he could not miss fractals.

The unconventional subtitles of this paper originate from H. Laul's interest in the world of music, where fractal structures have also widely been used [7].

References

1. Mandelbrot B.B. Les Objets fractals: forme, hasard et dimension. Flammarion: Paris, 1975, 365 p.
2. Peitgen H.-O. and Richter P.H. The Beauty of Fractals. Images of Complex Dynamical Systems. Springer: Berlin et al, 1986, 200 p.
3. Hubbart J. (communication at his seminar in DAMTP, University of Cambridge, Nov. 13th, 1989).
4. Mandelbrot B.B. The Fractal Geometry of Nature. Freeman: San Francisco, 1982.
5. Mandelbrot B.B. Fractals, in Encyclopedia of Physical Science and Technology, 1987, p. 579.
6. Feder J. Fractals. Plenum Press: New York and London, 1988, 284 p.
7. Peitgen H.-O. and Saupe D. (eds). The Science of Fractal Images. Springer: New York et al, 1988, 312 p.
8. Klieger P. Concrete, in McGraw-Hill Encyclopedia of Science and Technology, 1977, vol. 3, p. 399.
9. Лаул Х. Исследование железобетонных оболочек в Эстонской ССР. Изв. АН ЭССР, Сер. физ.-мат. и техн. наук, 1965, 14, № 3, с. 328-336.
10. Kantor Y. Energetic and entropic elasticity of the Sierpinski gasket. Physica D, 1989, 38, No. 1-3, p. 215-220.
11. Edwards S.F. and Oakeshott R.B.S. The transmission of stress in an aggregate. Ibid, p. 88-92.

12. Hermann H.J. Fractal deterministic cracks. Ibid, p. 192--197.
13. Mackay A.L. The Harvest of a Quiet Eye. Inst. of Physics: London and Bristol, 1988, 192 p.

J. Engelbrecht

FRAKTALID INSENERITEADUSES

Artikkel käsitleb fraktalite teooria põhimõisteid, mis võiksid olla rakendatud raudbetoonkonstruktsioonide ja eriti raudbetoonkoorikute projekteerimisel. Üks põhilisi küsimusi on pragude modelleerimine raudbetoonkonstruktsioonide tõmbele töötavates elementides. Lühidalt on kirjeldatud diskreetsetel elementidel põhinevat teooriat, mis võimaldab teatud ligikaudsusega modelleerida prao arenemist. Püstitatakse rida probleeme, mille lahendamiseks on kohane kasutada fraktalite teooriat.

Nr. 721

TALLINNA TEHNIKAÜLIKOOLI TOIMETISED
TRANSACTIONS OF TALLINN TECHNICAL UNIVERSITY

UDC 624.074

V. Kulbach

HANGING ROOFS AS ACOUSTIC SCREENS FOR SONG FESTIVAL TRIBUNES IN ESTONIA

Song festivals are a 120 years tradition in Estonia. The number of choir singers has grown to 30 thousand and the audience to 200 thousand people. Last years have seen increasing importance of song festivals, being driven by the movement for independent Estonia outside the Soviet Union. For example, in the "singing revolution" of 1988 every fourth Estonian took part.

A contemporary song festival tribune was erected in Tallinn in 1960. Architect Alar Kotli and Professor Heinrich Laul made a major contribution to the design of the acoustic screen. This screen is a saddle-formed hanging roof, one of the first examples of that kind. Because Tartu, the Estonian University town has a special place in the festival tradition, a new song festival tribune has been designed to be erected there. This acoustic screen is also a hanging roof with negative Gaussian curvature. The acoustic factor is domineering in the design of the screen surface. Both screens are inclined in the direction of the audience. The function and general shape of the screens in Tallinn and Tartu are identical, yet their structures are considerably different.

The prestressed cable network used in Tallinn is formed inside the contour, consisting of two plane arches (Fig. 1). The back arch is made of reinforced concrete, the plane being inclined at the angle of 19° to the horizon. The front arch consists of a steel tube, partly filled with concrete, inclined at the angle of 58° to the horizon. Both the back and the front arches have common main sup-

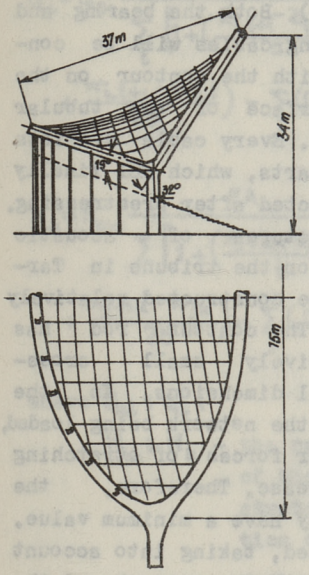

Fig. 1

ports in the form of massive counterforts, which develop considerable horizontal reactions to the arch forces. The back arch is complementarily supported by vertical columns of the rear wall of the tribune. At the same time, the front arch has no intermediate supports, therefore it has to resist not only the moments applied in its plane, but the perpendicular forces as well. Network cables are made of locked-coil wire ropes 38.5 mm in diameter. The bearing cables are joined at their upper ends to the outer surface of the front arch by means of bolt hinges. There are threaded elements, passing through the contour arches at the lower ends of bearing cables and both ends of stretching cables. Prestressing has been realized by screwing up the fastening screw nuts. In spite of relatively great bending rigidity of contour arches, the prestressing forces of the cables have remarkably great values (up to 300 kN). The roof of the screen consists of ribbed wooden panels, resting on the bearing cables.

The bearing structure of the acoustic screen of the tribune in Tartu is a hypar-formed network within a contour with a smoothly formed spatial axis, having elliptic and parabolic projections (Fig. 2). The contour will be constructed of a number of straight tubular sections and supported by three plain supports, connected with the contour and the foundation by linear hinges. Therefore, the supports do not resist symmetrical horizontal displacements of the contour. In this case, the interaction between the network and the contour is of particular importance when outer loads are balanced. The network is made of cables

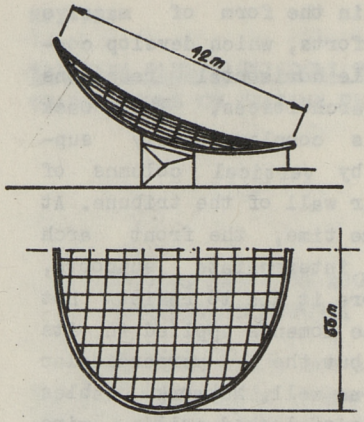

Fig. 2

of carbon round steel (32 mm in diameter). Both the bearing and stretching cables will be connected with the contour on the outer surface of the tubular sections. Every cable consists of two parts, which will finally be connected after prestressing. The structures of acoustic screen for the tribune in Tartu can be constructed relatively easily. The contour rod has comparatively small cross-sectional dimensions. In the case of the network being loaded, the inner forces of stretching cables will increase rather than decrease. Therefore, the prestressing forces of the network may have a minimum value. However, the screen has been calculated, taking into account the co-operation of the wooden roof with the network and the contour. To determine the stress — strain state within the network we have to proceed from the equilibrium conditions and the geometrical equations. For a network surrounded by two plane arches, it is convenient to use the algebraic equations suited for a limited number of cables. The total number of equations is five times the number of nodes. For an orthogonal network, the system of equations may be considerably simplified, consisting of a condition of equilibrium and two equations of geometrical compatibility for every node. Deflections of the contour nodes may be regarded as linear functions of the inner forces of the cables, using the corresponding influence lines for displacements of the contour. Thus we may write

$$w_{i,k}=\frac{1}{2\left(1+\frac{H_k a}{G_i b}\right)}\left[\left(w_{i,k-1}+w_{i,k+1}\right)+\frac{H_k a}{G_i b}\left(w_{i-1,k}+w_{i+1,k}\right)+\left(z_{i,k-1}-\right.\right.$$

$$\left.\left.-2z_{i,k}+z_{i,k+1}\right)+\frac{H_k a}{G_i b}\left(z_{i-1,k}-2z_{i,k}+z_{i+1,k}\right)-\frac{P_{i,k} a}{G_i}\right]; \qquad (1)$$

$$G_i = G_{0i} \frac{EA_i}{\sum_{\ell} \left[1+\left(\frac{z_{i,\ell+1}-z_{i,\ell}}{a}\right)^2\right]^{3/2}} \left[\sum_{\ell} \frac{w_{i,\ell+1}-w_{i,\ell}}{a}\left(\frac{z_{i,\ell+1}-z_{i,\ell}}{a} + \right.\right.$$

$$\left.\left. + \frac{w_{i,\ell+1}-w_{i,\ell}}{2a}\right) - \sum_{j}(G_j - G_{0j})\eta_{i,j} - \sum_{\ell}(H_\ell - H_{0\ell})\eta_{i,\ell}\cos\alpha\right]; \quad (2)$$

$$H_k = H_{0k} \frac{EA_k}{\sum\left[1+\left(\frac{z_{j+i,k}-z_{j,k}}{b}\right)^2\right]^{3/2}} \left[\sum_{j} \frac{w_{j+1,k}-w_{j,k}}{b}\left(\frac{z_{j+i,k}-z_{j,k}}{b} + \right.\right.$$

$$\left.\left. + \frac{w_{j+1k}-w_{jk}}{2b}\right) - \sum_{j}(G_j - G_{0j})\frac{\eta_{k,j}}{\cos\alpha} - \sum_{\ell}(H_\ell - H_{0\ell})\eta_{k,\ell}\right] \quad (3)$$

where G_{0i} ; G_i ;

H_{ok}; H_k - the respective projections of the forces of the i-th carrying cable and the k-th stretching cable before and after application of the system of external loads $P_{i,k}$;

$w_{i,k}$ - deflection of the node i, k induced by external loads;

$z_{i,k}$ - ordinate of the noad i, k before application of external loads;

η_{ij} ; $\eta_{i,\ell}$ - ordinates of the influence lines of displacements of the i-th point of the contour in the plane of j-th carrying and ℓ-th stretching cable respectively;

α - the angle of the inclined plane of the contour arches.

For a hypar-formed roof with elliptic-parabolic contour the network can be presented as a continuous surface, formed by a doubled family of parabolic cables. The conditions of equilibrium for the unloaded network are satisfied a priori: uniformly distributed contact load corresponds to the parabolic form of both bearing and stretching cables. The initial form of a prestressed hypar-network may be presented by the formula

$$z = f_x \frac{x^2}{a^2} - f_y \frac{y^2}{b^2} \quad (4)$$

The initial forces of bearing and stretching cables have respectively the values

$$G_0 = \frac{p_0 a^2}{2f_x} \quad \text{and} \quad H_0 = \frac{p_0 a^2}{2f_y}$$

where p_0 - the contact load between bearing and stretching cables, reduced to the unit area of the roof.

In the following we will suppose that the contour is connected with the foundation by vertical columns. In this case the extreme bending moments of the contour [1] may be presented in the form

$$M_{x=0} = \left[G_0(1-k^2) - H_0\right] \frac{a^2}{2} \left[\frac{(1-k^2)K(k)}{3k^2E(k)} - \frac{1+k^2}{3k^2}\right] \qquad (6)$$

$$M_{x=a} = \left[G_0 - H_0(1-k^2)\right] \frac{a^2}{2} \left[\frac{(1-k^2)K(k)}{3k^2E(k)} - \frac{1-2k^2}{3k^2}\right] \qquad (7)$$

where $k^2 = 1 - \frac{b^2}{a^2}$;

$E(k)$; $K(k)$ - elliptical integrals of the second grade.

The corresponding normal forces of the contour

$$N_{x=0} = G_0 b \quad \text{and} \quad N_{x=a} = H_0 a \qquad (8)$$

The behaviour of the network and the contour depends greatly on the relation between the curvatures of bearing and stretching cables $\alpha = f_y / f_x$. With the given α the maximum bending moments of the contour may take place both in the state of network loading and in prestressing. So, for the prestressing state the maximum contact load p_0 has to be restriced. In most cases, however, the contact load may have a comparatively small value without its going out when loading the roof by external loads.

When approximating the deflection form $w = w(x,y)$ of the network by function

$$w = w_0\left(\frac{x^2}{a^2} + \frac{y^2}{b^2} - 1\right) \qquad (9)$$

and applying it to the condition of equilibrium and to the equation of geometrical compatibility, we obtain an approximate cubic equation [2] for determining the deflection w_0:

$$(1+\psi+4\xi)\zeta_0^3+3\left[1-\alpha\psi+2(1-\alpha)\xi\right]\zeta_0^2+\left\{2\left[1+\alpha^2\psi+\right.\right. \tag{10}$$

$$\left.\left.+(1-\alpha)^2\xi\right]+p_0^*\left[1+(1+\frac{1}{\psi})\xi\right]\right\}\zeta_0=p^*\left[1+(1+\frac{1}{\psi})\xi\right]$$

where $\zeta_0=\frac{w_0}{f_x}$ - the relative deflection of the network;

$\psi=\frac{a^4t_x}{b^4t_y}$ - geometrical parameter;

t_x, t_y - effective thicknesses of the families of bearing and stretching cables, correspondingly;

$p^*=\frac{9pa^4}{10Et_xf_x^3}$ - the load factor;

$p_0^*=\frac{9p_0a^4}{10Et_xf_x^3}\left(1+\frac{1}{\alpha}\right)$ - the prestressing factor;

$\xi=\frac{5Et_ya^3(a/b)^{1/2}}{9\pi E_ct_cd_c^3}$ - the rigidity factor of the contour tube;

t_c and d_c - thickness and diameter of the contour tube;

E and E_c - modulus of elasticity of cables and contour material, respectively.

Formula (10) has been derived in view of displacements of the elliptical contour as a geometrically and physically linear curved rod, loaded by horizontal forces of bearing and stretching cables and using integration of the geometrical equations

$$\frac{\partial u}{\partial x} + \frac{\partial w}{\partial x}\left(\frac{\partial z}{\partial x} + \frac{1}{2}\frac{\partial w}{\partial x}\right) = \frac{\Delta G}{E t_x}\left[1 + \left(\frac{\partial z}{\partial x}\right)^2\right]^{3/2} \qquad (11)$$

$$\frac{\partial v}{\partial y} + \frac{\partial w}{\partial y}\left(\frac{\partial z}{\partial y} + \frac{1}{2}\frac{\partial w}{\partial y}\right) = \frac{\Delta H}{E t_y}\left[1 + \left(\frac{\partial z}{\partial y}\right)^2\right]^{3/2} \qquad (12)$$

where u and v - horizontal displacements of the network,
ΔG and ΔH - the increase in forces of bearing and stretching cables, respectively.

To determine ΔG and ΔH we have nonlinear equations

$$\Delta G = \frac{5 E t_x f_x^2 \zeta_0 [(2+\zeta_0) + 2(1-\alpha+\zeta_0)\xi]}{9a^2[1+(1+\frac{1}{\psi})\xi]} \qquad (13)$$

$$\Delta E = \frac{-5 E t_y f_x^2 \zeta_0 [(2\alpha-\zeta_0) - \frac{2}{\psi}(1-\alpha+\zeta_0)\xi]}{9b^2[1+(1+\frac{1}{\psi})\xi]} \qquad (14)$$

The bending moments and corresponding normal forces in the contour may be expressed by equations (6), (7) and (8) when replacing the values G_0 and H_0 by summarized forces $G = G_0 + \Delta G$ and $H = H_0 + \Delta H$.

The smaller the maximum value of the bending moment of the contour, the smaller is the rigidity of the contour in bending (the bigger is the rigidity factor ξ).

The approximate deflection function (9) assumes that displacements w on the contour curve have zero value. Our experimental investigations on the model of the acoustic screen for the tribune in Tartu have proved that the given system of equations is applicable to the hanging roofs with partly supported contour [2]. A slight inclination does not also bring about considerable changes of network deflections and inner forces. So, taking into account the given parameters

$a = 21\,m$, $b = 27\,m$, $f_x = 4{,}2\,m$, $f_y = 2{,}8\,m$, $d_c = 1{,}21\,m$,

$t_c = 16\,mm$, $t_x = t_y = 0{,}471\,mm$, $p = 1{,}5\,kN/m^2$, $p_0 = 0{,}3\,kN/m^2$,

$E = E_c = 0{,}21 \times 10^6\,MPa$

we have $\zeta_0 = 0{,}179$, $G = 128\,kN/m$, $H = 121\,kN/m$ and

the calculated maximum inner forces in the contour

$$M = 3497\ kN{:}m,\quad N = 3456\ kN$$

The maximal stresses in the contour tube $\sigma = 293$ MPa, in the cables $\sigma = 451$ MPa correspond satisfactorily to the experimental values.

References

1. Laul H. and Kulbach V. Analysis of cable network with negative Gaussian curvature. J. of Structural Mechanics (Finland), 1974, Vol. 7, No 1, pp. 3-18.
2. Kulbach V. Behaviour of tubular contour of hypar-formed hanging roofs. International Symposium on Tubular Structures. Preprints. Lappeenranta, Finland, 1989, pp. 7.06--1-7.06.-6.

V. Kulbach

RIPPKATUSED LAULULAVA AKUSTILISTE EKRAANIDENA EESTIS

1960. aastal valminud Tallinna laululava ning 1989. aastast ehitatava Tartu laululava akustilised ekraanid kujutavad endast erinevaid sadulakujulisi rippkatuseid. Tallinna ekraani kontuur koosneb kahest tasapinnalisest kaarest ning on toetatud massiivsetele kontraforssidele. Tartu ekraani kontuur on plaanis ellipsikujuline ruumne kinnine kõver, mis toetub kolmele tasapinnalisele vertikaalsele diafragmale. See ei takista kontuuri kujumuutust horisontaalsuunas. Samuti esineb olulisi erinevusi vantidevõrgu kujundamisel ning vantide kinnitamisel kontuuri külge. Tartu ekraani iseärasuseks on ka eelpingejõudude oluliselt väiksemad suurused võrreldes Tallinna ekraaniga. Väiksemate eelpingejõudude kasutamist võimaldab asjaolu, et nii katuse kui ka kontuuri koormuste mõjul suurenevad kande- ja pingestusvantide sisejõud.

Artiklis on toodud seosed kummagi ekraani sisejõudude ja siirete määramiseks, lähtudes vastavalt diskreetsest või kontinuaalsest arvutusskeemist.

No 721

TALLINNA TEHNIKAÜLIKOOLI TOIMETISED
TRANSACTIONS OF TALLINN TECHNICAL UNIVERSITY

UDC 624.074

V. Kulbach, P. Paane

STATICAL TESTING OF AN ACOUSTIC SCREEN MODEL

Introduction

The acoustic screen for the song festival tribune in Tartu (Estonia) has been designed, forming a hypar-shaped suspended roof inside an inclined elliptical contour. The network is covered by a three-layer timber shell roof. The model was tested at the Laboratory of Lightweight Structures of Tallinn Technical University. In this paper the behaviour of the screen structure without the timber shell is analysed. Some problems related to mounting and prestressing have also been specified to verify dimensions of the network and the contour tube.

Model Description

The screen model (Fig. 1) was made in the scale of

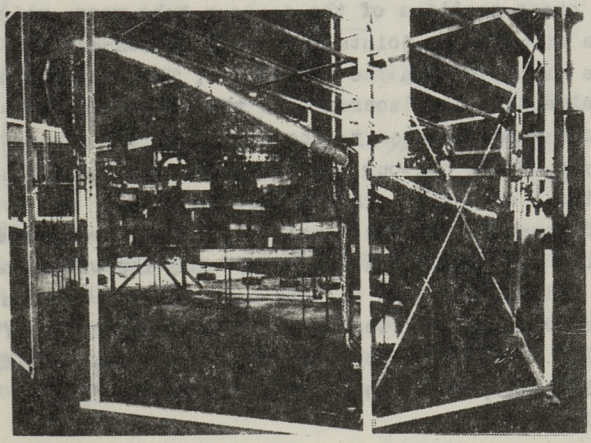

Fig. 1. Screen model

1:10. Butt joints were used to weld the contour rod, consisting of straight sections of tubes with the outer diameter of $D = 122$ mm and thickness of $t = 1.6$ mm. Longitudinal ribs with a cross-section of 1.6 x 20 mm for fastening the cables and the timber shell were welded to the inner side of the contour tube. Central points of cross-sections of the contour joints were located on a spatial curve, formed by crossing two surfaces: hypar

$$z = f_x \frac{x^2}{a^2} - f_y \frac{y^2}{b^2}$$

and an elliptical cylinder

$$\frac{x^2}{a^2} + \frac{y^2}{b^2} = 1$$

where

$$a = 2.1 \text{ m}, \quad b = 2.7 \text{ m}, \quad f_x = 0{,}4 \text{ m}, \quad f_y = 0.3 \text{ m}$$

were taken for the surface of the model.

The contour rod was rested on three plain supports, including two side and one back support. The contour had no supports in fore part. It was freely suspending and supported by the network only. Each support consisted of two tubular columns ($d = 51$ mm) and diagonal ties between them. To transmit loads from the contour to the columns, the supporting cross-sections of the contour tube were reinforced by cross ribs. Hinge joints were used to connect the columns with the ribs and with the foundation. This supporting system enables free displacements of the supported parts in the directions perpendicular to the plains of the supports. The front part of the contour may freely be displaced also in the vertical direction. The network consisted of two families of parabolic cables, including wires with the diameter of $d = 3$ mm and spacing of 150 mm. The wires of the network had pressed tags on both ends, which were connected with the longitudinal ribs of the contour by means of hinge bolts. The length of every cable may be regulated with a threaded thrust, thus enabling to verify the form of the roof surface.

Investigation Techniques

Different gravitational loads were used for loading purposes, and were applied to the nodes by means of a multistage lever system, enabling network loading by the desired combination of loads applied on every quarter of its surface. Examples of loading are given in Table 1. Additional loads were used to simulate the weight of the contour rod and were uniformly distributed over the length of the contour (0,45 kN/m for the empty tube and 2,89 kN/m for the tube filled with concrete).

TABLE 1

Loading case	Distributed surface load on the quarters of the network [kPa] 1)				The length of the concrete-filled part of the contour [m] 2)
	I	II	III	IV	
A 1	0.90	0.90	0.90	0.90	---
A 2	1.62	1.62	1.62	1.62	---
B 1	0.90	1.48	1.48	0.90	---
B 2	0.90	1.48	1.48	0.90	0.65
B 3	0.90	1.48	1.48	0.90	1.30
C 1	0.90	0.90	---	---	---
C 2	0.90	1.48	---	---	---
D 1	---	---	---	---	3)
E 1	---	---	---	--- 4)	0.55
E 2	---	---	---	---	1.30
F 1	---	---	---	--- 5)	0.55
F 2	---	---	---	---	1.30

1) see Fig. 2
2) location of the load, modelling the weight of the concrete, see Fig. 2
3) distributed load over the length of the contour 0,45 kN/m
4) uniformly distributed load on the surface 0.12 kPa
5) uniformly distributed load on the surface 0.90 kPa

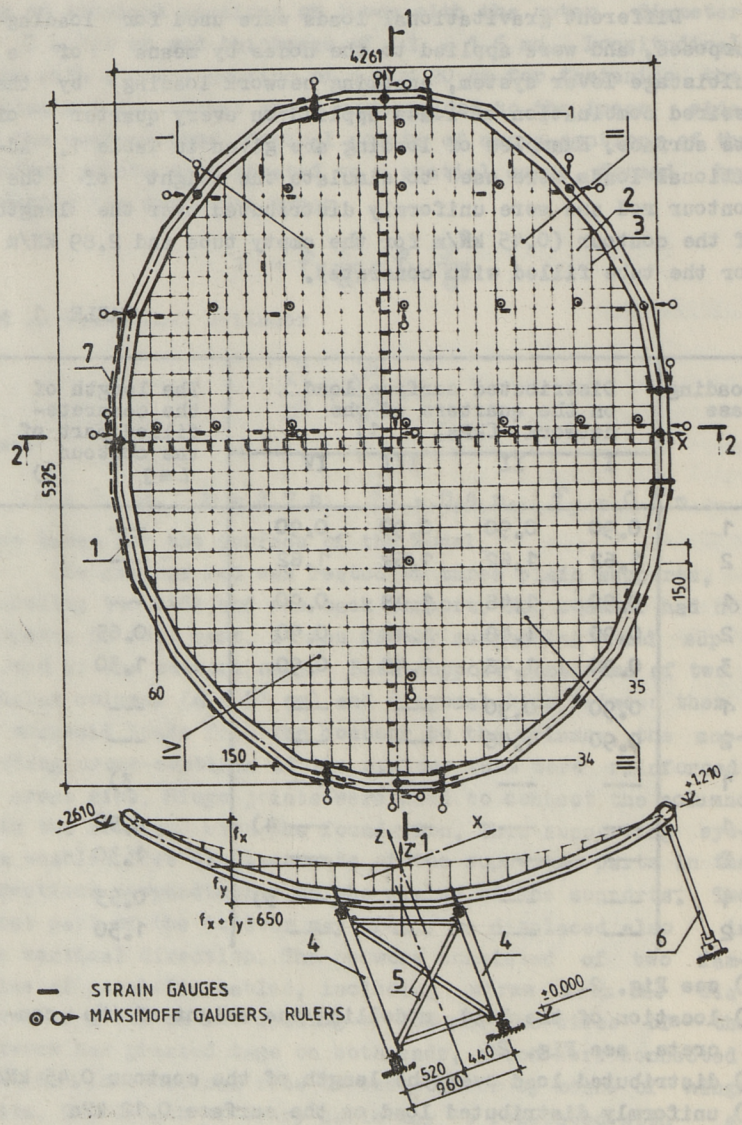

Fig. 2. Scheme of the model.
1 - contour; 2 - bearing cable; 3 - stretching cable;
4 - support columns; 5 - ties; 6 - support columns;
7 - location of the load, modelling the weight of concrete.

To measure the inner forces of cables and the stresses in the contour tube strain gauges bonded to the surface of the wire or the tube were used. Measuring instrument fixture ARMI-1, connected to CM-1800 computer, and the programming system ASTOR were made use of. Displacements of different cross-sections of the contour in the directions of axes x, y, z were measured by means of Maksimoff-gauger with the scale graduation of 0.1 mm. To measure the displacements of network nodes measuring rulers with the scale graduation of 1.0 mm were used. A spatial framework (Fig. 1) was built to fix the measuring instruments. Location of strain and displacement gauges is shown in Figure 2.

Strains and displacements were measured in great detail on a half the network. At the same time, to fix possible nonsymmetry of the measurements, double measuring was partially used.

Test Results

After prestressing by contact load $p_o = 0.15$ kN/m^2 we obtained the actual rises $f_x = 373$ mm and $f_y = 246$ mm ($f_x/f_y = 1.516$), when the contour was loaded by 0.45 kN/m the inner forces within cables ranged from 0.06 to 0.14 kN. By all kinds of loading, as demonstrated in Table 1, an increase of inner forces both in bearing and in stretching cables was observed. The plots of Figures 3, 4, 7 and 8 show an increase in inner forces under the action of loads. The family of bearing cables falls under enumeration from 1st to 34th and that of stretching cables from 35th to 60th.

To shorten the bending moments in the contour, it is advisable to use filling with concrete in some parts of the contour tube.

The diagrams in Figures 9 and 10 demonstrate the distribution of the bending moments of the contour. The maximal values of the moments may be observed above the back and side supports and also in the middle of the suspending front part. The influence of the weight of concrete filling inside the front part of the contour tube may be illustrated by Figures 5, 7, 8, 9 and 10. Loading by the weight of concrete leads to an increase of the inner forces in both cable families.

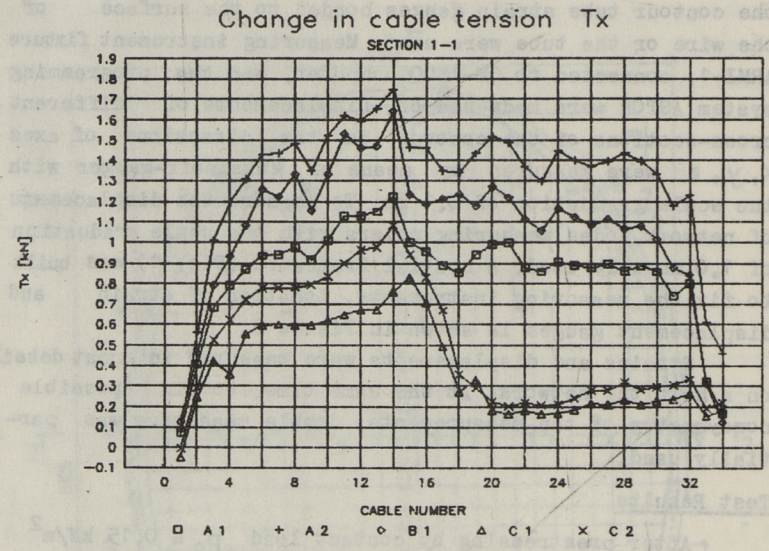
Change in cable tension Tx
SECTION 1–1
Tx [kN]
1.9
1.8
1.7
1.6
1.5
1.4
1.3
1.2
1.1
1
0.9
0.8
0.7
0.6
0.5
0.4
0.3
0.2
0.1
0
−0.1
0
4
8
12
16
20
24
28
32
CABLE NUMBER
A 1
A 2
B 1
C 1
C 2

Fig. 3

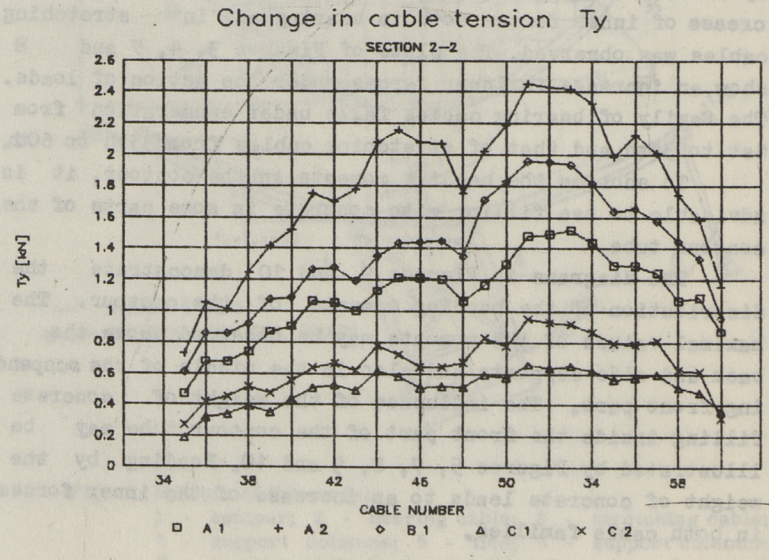
Change in cable tension Ty
SECTION 2–2
Ty [kN]
2.6
2.4
2.2
2
1.8
1.6
1.4
1.2
1
0.8
0.6
0.4
0.2
0
34
38
42
46
50
34
58
CABLE NUMBER
A 1
A 2
B 1
C 1
C 2

Fig. 4

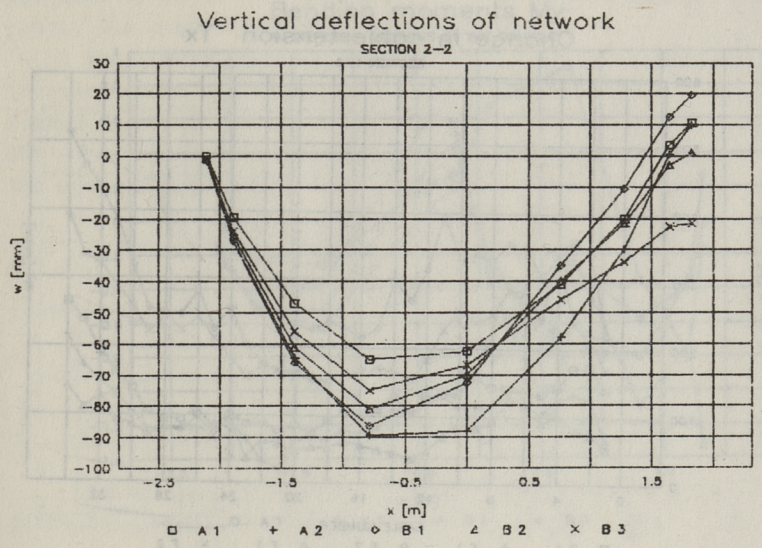
Vertical deflections of network
SECTION 2–2
w [mm]
x [m]
A 1
A 2
B 1
B 2
B 3

Fig. 5

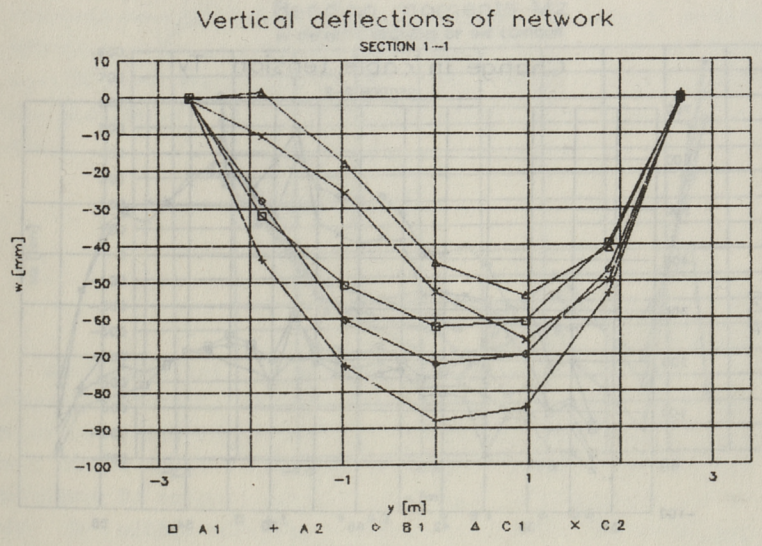
Vertical deflections of network
SECTION 1–1
w [mm]
y [m]
A 1
A 2
B 1
C 1
C 2

Fig. 6

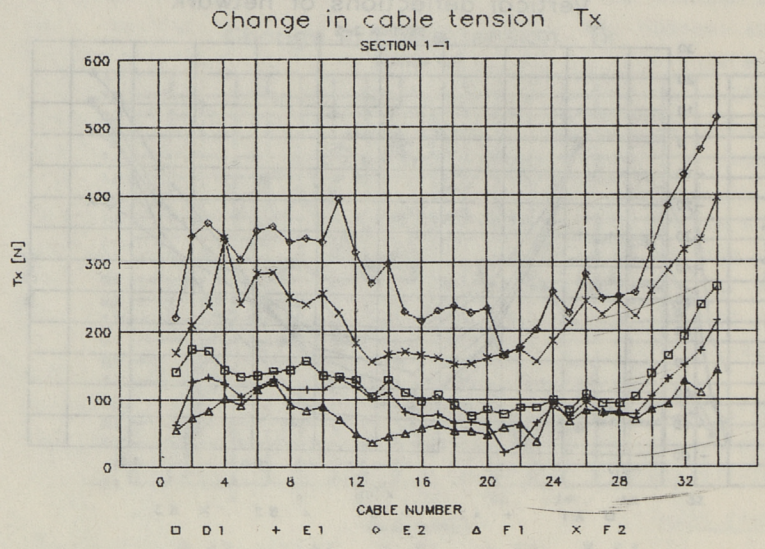
Change in cable tension Tx
SECTION 1–1
600
500
400
300
200
100
0
Tx [N]
0
4
8
12
16
20
24
28
32
CABLE NUMBER
D1
E1
E2
F1
F2

Fig. 7

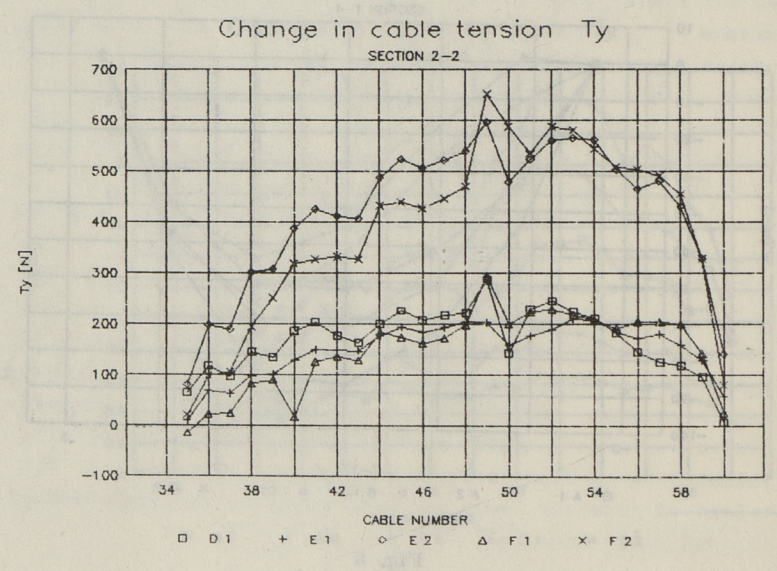
Change in cable tension Ty
SECTION 2–2
700
600
500
400
300
200
100
0
−100
Ty [N]
34
38
42
46
50
54
58
CABLE NUMBER
D1
E1
E2
F1
F2

Fig. 8

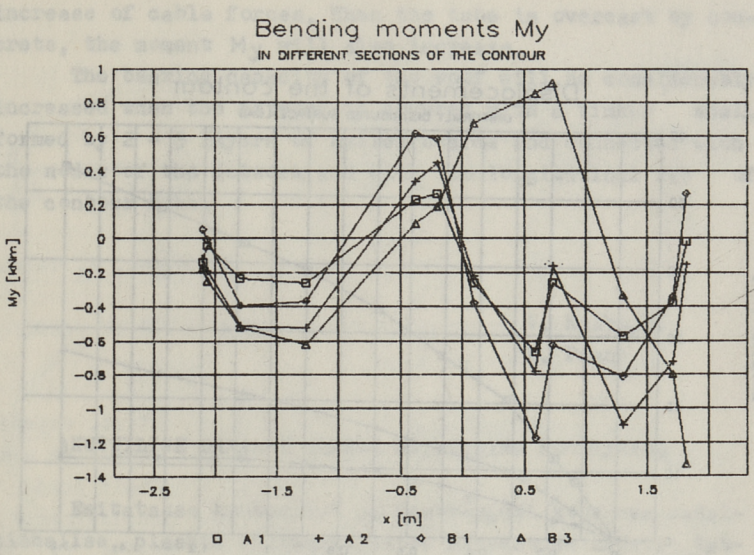
Bending moments My
IN DIFFERENT SECTIONS OF THE CONTOUR
My [kNm]
1
0.8
0.6
0.4
0.2
0
−0.2
−0.4
−0.6
−0.8
−1
−1.2
−1.4
−2.5
−1.5
−0.5
0.5
1.5
x [m]
A 1
A 2
B 1
B 3

Fig. 9

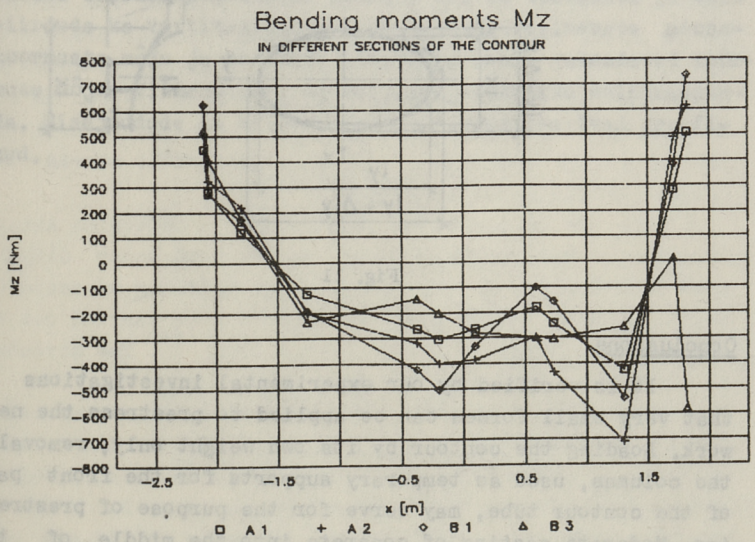
Bending moments Mz
IN DIFFERENT SECTIONS OF THE CONTOUR
Mz [kNm]
800
700
600
500
400
300
200
100
0
−100
−200
−300
−400
−500
−600
−700
−800
−2.5
−1.5
−0.5
0.5
1.5
x [m]
A 1
A 2
B 1
B 3

Fig. 10

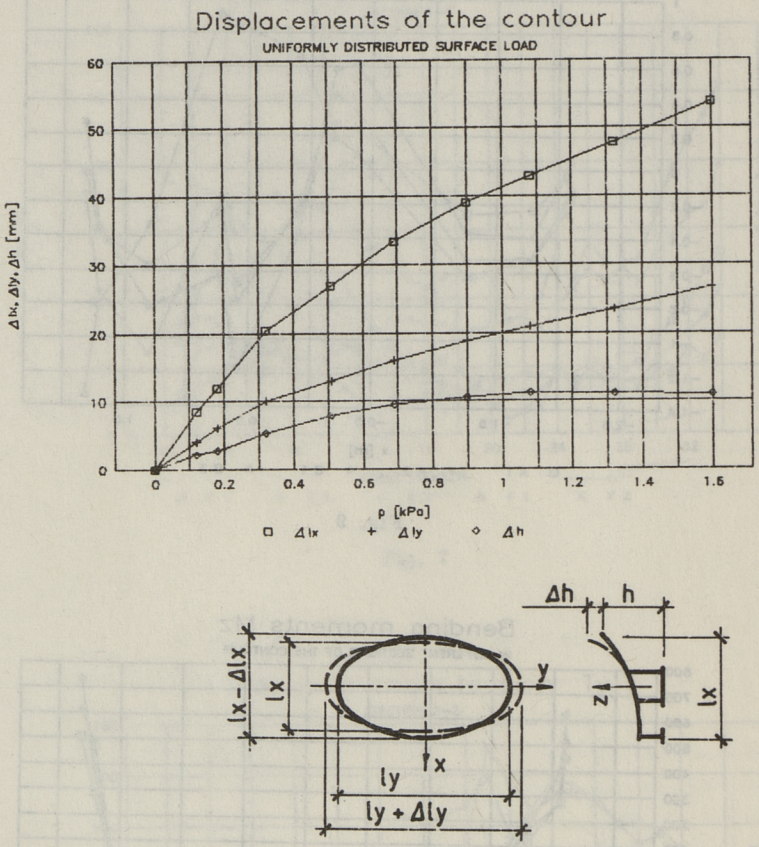

Fig. 11

Conclusions

It is verified by our experimental investigations that very small forces can be applied to prestress the network. Loading the contour by its own weight only, removal of the columns, used as temporary supports for the front part of the contour tube, may serve for the purpose of prestressing. Moderate casting of concrete into the middle of the front part of the tubular contour brings about a decrease of the bending moments M_y, but it is accompanied by an

increase of cable forces. When the tube is overcast by concrete, the moment My will also increase.

The bearing capacity of the roof will be considerably increased when the network is covered with a timber shell, formed by 2 - 3 layers of nailed boards and connected with the nodes of the network and with the longitudinal rib of the contour tube.

V. Kulbach,
P. Paane

AKUSTILISE EKRAANI MUDELI STAATILINE KOORMAMINE

Esitatakse kontuurist ja vantvõrgust koosneva sadulpinnalise, plaanis ellipsikujulise rippkatuse mudeli katselise uurimise tulemused. Mudel on valmistatud mõõtkavas 1:10, ellipsi poolteljed 2,7 m ja 2,1 m. Kate toetub kolmele paaristoele, mis võimaldavad kontuuri norisontaalsuunalisi siirdeid. Kontuuri eesmine osa on toetamata ja võib siirduda ka vertikaalsuunas. Vaadeldakse erinevate pinnakoormuste mõju ja kontuuri eesmisele osale rakendatud koormuse mõju. Viimase abil on võimalik vantvõrku eelpingestada. Sisejõudude ja siirete jaotust illustreerivad graafikud.

No 721

TALLINNA TEHNIKAÜLIKOOLI TOIMETISED
TRANSACTIONS OF TALLINN TECHNICAL UNIVERSITY

UDC 624.074

K. Õiger, I. Talvik

DETERMINATION OF DYNAMIC CHARACTERISTICS OF SADDLE-SHAPED SUSPENSION ROOF

When designing large-span suspension systems, especially if dead load is relatively small, special attention should be paid to live loads. As wind belongs to dynamic loads, the magnitude of wind-induced inner forces and displacements of flexible structures depends on dynamic properties of the structure. Dynamic properties are characterized by natural modes, frequencies and damping factors. In this article the free-vibration behaviour of a saddle-shaped suspension roof with an elliptical contour will be examined. The contour of the roof, freely deformable in a horizontal plane, is supported only in vertical direction by three pin-ended plane supports, supplying stability for the whole system. The roof surface is formed by pretensioning an orthogonal steel rod net within the contour. A 3-layer timber shell serves the purpose of cladding on the net.

The aim of our investigation was to determine natural frequencies and damping factors of the roof under different load conditions both with and without cladding to estimate sensibility to vibrations. The studies were carried out with a 1:10 scale model of the prototype (Fig. 1). The structure is thoroughly described in [1].

The dynamic characteristics were determined by recording the oscillations of cable deformations and displacements of the network at different locations in the conditions of damped free vibrations of the structure (Fig. 2). If the structure executes vibrations according to one of its natural modes, the recorded displacements at different points of the roof follow one-component damped harmonic vibrations. In this

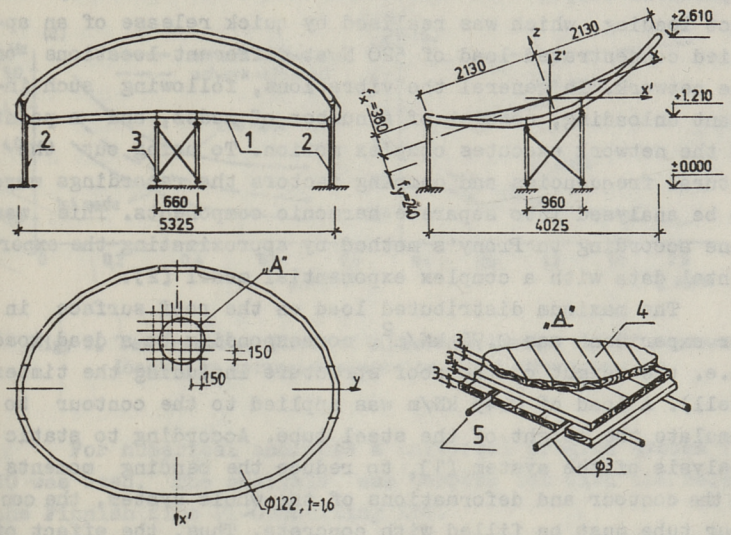

Fig. 1. Scheme of the model.
1 - contour; 2, 3 - supports; 4 - timber shell;
5 - cables.

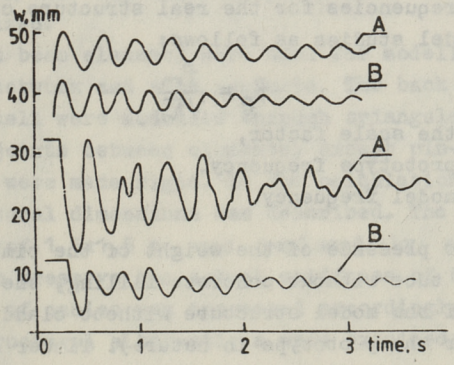

Fig. 2. Examples of recorded displacements.
A - network without shell; B - network with timber shell.

experiment damped free vibrations were also excited by impact loading, which was realised by quick release of an applied concentrated load of 520 N at different locations on the network. In general the vibrations, following such instant unloading, consist of a number of modes, and a point of the network executes complex motion. To bring out the natural frequencies and damping factors the recordings were to be analysed into separate harmonic components. This was done according to Prony's method by approximating the experimental data with a complex exponential model [2].

The maximum distributed load on the roof surface in our experiment was 0.70 kN/m^2, corresponding to a dead load (i.e. the weight of the roof structure including the timber shell). A load of 0.45 kN/m was applied to the contour to simulate the weight of the steel tube. According to static analysis of the system [1], to reduce the bending moments in the contour and deformations of the whole system, the contour tube must be filled with concrete. Thus, the effect of the contour weight on dynamic characteristics of the system was also studied. In experiments on the model with timber shell, the contour load reached the value of 2.08 kN/m to model the own weight of the concrete-filled sections of the contour tube.

The results of the tests are presented in Fig. 3. The prototype frequencies for the real structure can be obtained from the model studies as follows:

$$f_p = \frac{f_m}{\sqrt{\lambda}}$$

where λ - the scale factor,
f_p - prototype frequency,
f_m - model frequency.

In the presence of the weight of the timber shell and the contour tube without concrete filling, the fundamental frequency of the model structure without cladding is 2.98 Hz (0.81 Hz for the prototype in nature). Timber shell increases the frequency up to 3.20 Hz (1.01 Hz in nature). The first two frequencies of the model with the timber shell and the weight of the concrete-filled contour are 2.45 Hz (0.77 Hz) and 4.74 Hz (1.50 Hz).

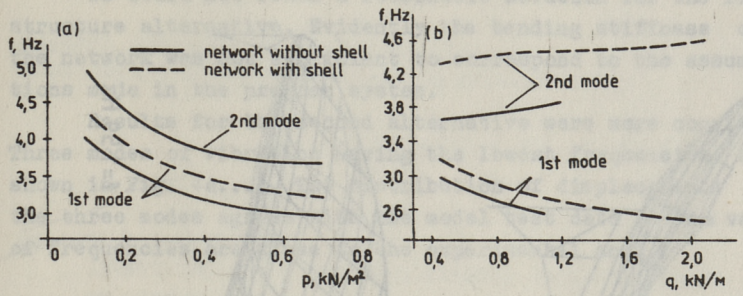

Fig. 3. Test results. Effect of (a) surface loading and (b) contour loading on natural frequencies of the structure.

For numerical analysis a universal program system TPS-10 was used. The analysis was carried out with the help of the Finnish firm PI-Consulting Ltd.

TPS-10 is based on the finite element method and the realized version used geometrically linear theory. We assumed the amplitudes of vibration to be relatively small and so the naturally nonlinear behaviour of the structure to be negligible for determining the natural frequencies. At the same time linear theory is easier to handle for such a complex structure, and expensive computer time can be significally economized.

Straight beam elements were used for modelling the contour, cable network and side supports. The back supports and the timber shell were modelled through triangular plate elements. All joints between elements, except pin-jointed support-columns were made rigid. In the calculations the structure with natural dimensions was described. The real network with a pitch of 1.5x1.5 m was replaced by a network of 4.5x4.5 m. To preserve the actual stiffness of the network, the diameter of cables was increased accordingly.

Two structural alternatives were examined:

- cable network without a timber shell, a contour without concrete filling, vibrating mass on the network simulating the mass of the roof with timber shell;

- cable network with a timber shell and contour filled with concrete.

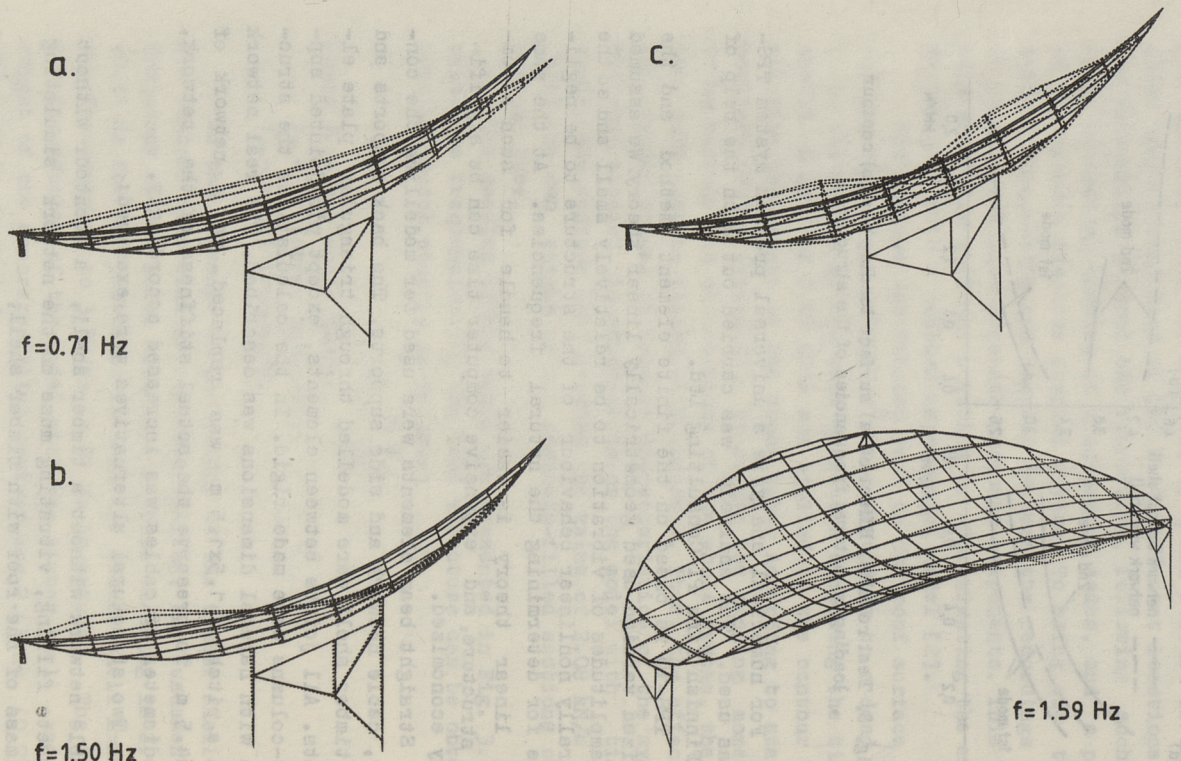

Fig. 4. Computed mode shapes.

We could not reach a reasonable solution for the first structure alternative. Evidently the bending stiffness of the network was not sufficient to correspond to the assumptions made in the program system.

Results for the second alternative were more convincing. Three modes of vibration having the lowest frequencies are shown in Fig. 4a...c. The distribution of displacements of the three modes agrees with the model test data and the values of frequencies are close to the experimental ones.

Conclusions

The lowest frequency of natural vibrations of the examined structure is to a great degree determined by the mass of the freely suspending front part of the contour. So in designing a real structure it is necessary to take into consideration, that an increase of the system's static stiffness with a simultaneous increase of its own weight may cause a considerable decrease of the natural frequencies of the structure.

Restrained changing of network weight does not substantially influence the frequencies of the first two modes.

No significant influence of the presence of cladding or the changes in loads on the damping characteristics was observed. The average value of logarithmic decrement of vibration was 0.18.

Using the finite element method enables to determine the lowest natural frequencies of the complex structure (consisting of contour, cable net and timber shell) with acceptable accuracy.

References

1. Kulbach V., Paane P. Statical Testing of an Acoustic Screen Model. Transact. Tallinn Tech. Univ. 1990, No 721, p. 21-31.
2. Marple S.L. Digital Spectral Analysis and Its Applications. Prentice-Hall, N.Y., 1987.

K. Õiger, I. Talvik

SADULAKUJULISE RIPPKATTE DÜNAAMILISTE PARAMEETRITE MÄÄRAMINE

Artiklis on esitatud kontuurist ja ortogonaalsest vantvõrgust koosneva sadulpinnalise, plaanis ellipsikujulise rippkatte võnkumiskatsete tulemused. 1:10 mõõtkavas mudeli poolteljed on 2,7 m ja 2,1 m. Kontuur toetub kolmele tasapindsele paaristoele, mis võimaldavad kontuuri horisontaalsuunalisi siirdeid. Kontuuri eesmine osa on toetamata. Kattekonstruktsiooniks on kolmekihiline puitkoorik. Vaadeldakse erinevate pinna- ja kontuurikoormuste ning kattekonstruktsiooni mõju omavõnkesagedusele. Määratud on ka konstruktsiooni sumbumise logaritmiline dekrement. Numbriliselt määratud omavõnkesagedused puitkoorikuga kaetud konstruktsiooni puhul on lähedased eksperimendi tulemustele.

No 721

TALLINNA TEHNIKAÜLIKOOLI TOIMETISED
TRANSACTIONS OF TALLINN TECHNICAL UNIVERSITY

UDC 624.074.4.012.45.001.5 (474.2)

Ü. Tärno

INVESTIGATION OF DOUBLE-CURVATURE SHELLS BY MEANS OF MODELS

During 1955 - 1975 a great number of experimental and theoretical investigations [1, 2] were realized by the members of the scientific school of Professor Heinrich Laul, the academician of the Estonian Academy of Sciences, under his direction and supervision. The investigations allowed to reach some generalizations on the shells of natural material (reinforced concrete) in the state of cracks. This experience was specified during the next 10 years by studying various double curvature shells in the elastic and cracked states in a wide scale of geometrical parameters.

In the course of the last few years numerous experiments with fiberglass plastic thin-walled shells have been carried out in Tallinn Technical University. The studied fiberglass plastic ($E \simeq 20$ GPa) is made on the basis of polyester resin (40 %) and glass fibre (60 %). Some (> 10) layers of glass fibre (with various directions) have been used to make the shell material isotropic [3].

Smooth and ribbed shell models have been investigated, with positive ($R_1 / R_2 > 0$), zero ($R_1 / R_2 \to \infty$) and negative $R_1 / R_2 < 0$) Gaussian curvatures (Fig. 1), on rectangular plan in elastic state and in the state of discrete surface defects (line hinges, openings and hand-made cracks). Various prestressed cable systems have been used: straight prestressed cables near the fibre of the longitudinal edge beams, and supporting cables under the thin-walled part. The effect of various anchoring and fixing methods of prestressed cables on the distribution and quantity of inner forces has been investigated.

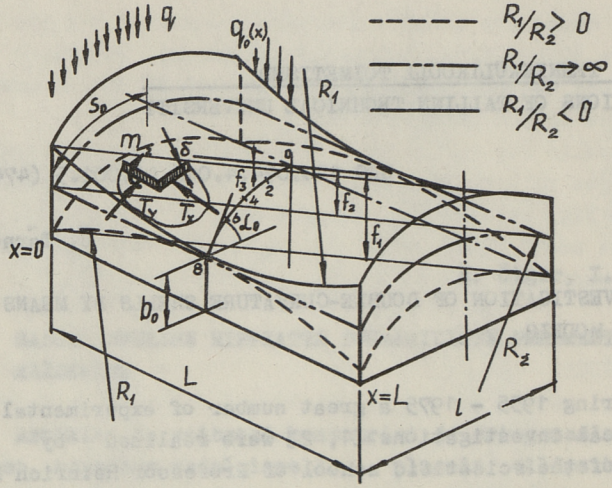

Fig. 1. Particulars of the studied shells.

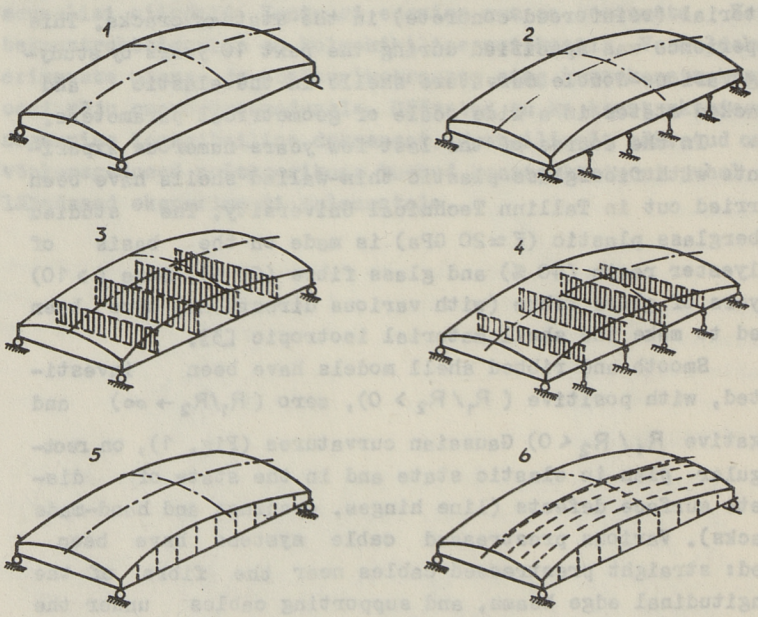

Fig. 2. Working schemes 1 - 6.

The papers [4, 5, 6] present the working peculiarities of middle-length cylindrical shells. Six working schemes have been investigated (Fig. 2). Schemes 5 and 6 describe the shells with hand-made transverse and longitudinal cracks. The flexural and torsional rigidities are varied and the effect of the load and of the geometrical parameters on the distribution of inner forces is explained.

According to scheme 6 it becomes evident that the longitudinal cracks, caused by negative bending moments that are effected by eccentricity of transverse normal forces, have a non-essential influence on the distribution of inner forces. There is a remarkable increase of negative transverse bending moments of the span in the shells with low torsional rigidity of edge beams. An analogous tendency takes place in shells with decreasing height of the edge beams.

A certain portion of loads is directed on the intermediate supports if the shells have vertically supported edge beams. The most essential portion of loads is transferred to the additional supports if the shell works as a medium panel. It indicates the replacement of the shell work by the vault work in transverse direction.

Specific distribution of inner forces occurs in the case the inner vault panels are supported. The change of the sign of transverse bending moments and the decrease of the role of longitudinal normal forces take place.

The papers [7 - 12] present the working art of very flat shells ($R_1/R_2 = 5 - 10$) in the longitudinal direction with rectangular plan ($L/\ell = 2 - 3$). Different working schemes have been used.

The diagrams of longitudinal normal forces are characterized by the beginning of pressure zones directly at the longitudinal edge beams. The maximum of pressure exists near the quarter of a transversal span. In the ridge of the shells negative transverse bending moments dominate. Relatively long shells are characterized by a saddle-shape diagram of longitudinal normal forces. The transverse bending moments that depend on the height of the longitudinal edge beams are negative over the whole cross-section ex-

cept for a narrow zone at the edge beam.

The inner forces, however, are considerably influenced by edge conditions. The neutral line of the longitudinal normal forces moves to the quarter of the transversal span in the shells with vertically supported edge beams. The saddle shape of the diagram disappears. There is an increase in positive bending moments. Great changes take place in the inner forces of the shells of vertically supported inner panels (scheme 4).

The comparison of the experimental data of fiberglass-plastic and reinforced concrete shells allows us to conclude that the distribution of the inner forces in both series is analogous. The longitudinal distribution of longitudinal normal forces suggests a considerable influence of the diagonal arches on the work of unsupported edge beams.

In the longitudinal edge beams of cylindrical and quasicylindrical shells very large longitudinal normal tension forces exist. Due to these forces transversal tension cracks develop. A large area of negative transversal bending moments also forms in the ridge zone of the thin-walled part [13]. Prestressed cables call forth an increase of positive transversal bending moments in the ridge zones of the shell. It is possible to determine the prestressing forces to minimize negative transversal bending moments.

In [13, 14] graphs of inner forces for positive Gaussian curvature quasi-cylindrical shells with beam-like and arch-like edge beams are presented with straight prestressed cables near the lower fibre of the longitudinal edge beams. A high strength and a low Young modulus make it possible to change the shape of the transversal and longitudinal cross-sections and thus to change the distribution of the inner forces in the required direction.

It is possible to conclude that quasi-cylindrical shells of negative Gaussian curvature act under unfavourable conditions [15]. The distribution of the inner forces gives rise to a considerable change of basic geometrical parameters and so the static work of the ucture under load deteriorates remarkably. When the ratio of the radii of the principal curvatures R_1/R_2 decreases from 10 to 5, the

longitudinal inner force Tx can be a tensional one in the area of the ridge.

In combined shell structures, thin-walled panels are supported by prestressed longitudinal cables [16]. With the help of these prestressed cables we can change the geometry of the shell and thereby influence the main inner forces. The external loads are distributed between the cable net and the shell surface.

For large-span shells, a rib system connected with a thin-walled cylindrical plate for transmitting inner forces is to be used. It is possible to form precast shells with similar surfaces in the same mould in various positions, whereas ribs can be placed when or where necessary [17, 18]. Discrete reinforcement with orientated glass fibre or steel rods is also possible to use. In [17, 18] the data of fiberglass plastic cylindrical shells with different variants of transversal ribs on external and internal surfaces of the thin-walled part are also presented. With ribs on the internal surface, a considerable increase of positive transversal bending moments occurs.

Experiments have been made with smooth shells with discrete surface defects - line-hinges [19, 20, 21].

The formation sequence of the hand-made longitudinal cracks has been selected in correspondence with the bending moment diagram. The shell part between longitudinal cracks works in elastic stage and has great stiffness in comparison with line-hinges.

We started with a hand-made crack on the ridge of the shell. Longitudinal normal forces at that stage compared to these in elastic stage. The pressure decreases in the ridge zone, its maximum value moves in the direction of the longitudinal edge beam.

The negative bending moments decrease near the crack zone, but increase approaching the longitudinal edge beam. The maximum point of pressure moves in the direction of the edge beam in models with three and five hand-made cracks. When the whole cross-section (we had 7 line-hinges) is subjected to the influence of hand-made cracks, bending moments of similar values form in every point of the cross-section.

It has been observed that the eccentricity of transversal normal forces in the line cracks affect the moment state of the shells. Transversal forces have a very important role in transferring the bending moments across the unreinforced longitudinal cracks. It is possible to use the method of calculating the transversal normal force in shells with longitudinal cracks only when the shell becomes more convex under the load.

Some stress state problems in the corner zones of the shells with reinforced and unreinforced diagonal cracks have been dealt with. Fiberglass plastic models with handmade diagonal cracks have been used [22]. For the investigation of membrane inner forces and bending moments near the diagonal cracks special tensoresistor systems are used. In the state of zero diagonal crack there are two different parts in the shell. The distribution of inner forces in the lower part is close to that of the plate, while it is close to that of the arch in the upper part. We can draw a conclusion that there is no essential change of the principal inner force T_1 caused by the longitudinal forces T_x. The failure of the shell can be caused by the existing unreinforced diagonal cracks. The latter start evolution in the unreinforced zones and travel farther into the cylindrical part of the shell. It can be concluded that the transfer of the principal inner force T_1 by the unreinforced diagonal cracks does not take place. All these forces must be transferred by a special reinforcement.

In the papers [23, 24] some graphs and generalizations of the experimental results in a large diapason of geometrical and loading parameters of fiberglass plastic shells are presented.

The main inner forces for the design of shells [25] of average length are the total tensile forces, the transverse moments and the increase of the membrane shear in a fixed point of the cross-section. All these inner forces can be calculated using dimensionless parameters.

References

1. Tärno Ü. Õhukeseseinaliste raudbetoonkoorikute uurimiskoolkonnast (prof. H. Laulu koolkonnast) TPI-s. Tehnilise mõtte ja tehnikahariduse ajaloo probleeme Eestis. Vabariikliku konverentsi (20.-21. dets. 1984) materjalid II. Tallinn, 1985, lk. 139-145.
Investigations of Thin-walled Concrete Shells (the Prof. H. Laul School).

2. Tärno Ü. Raudbetoonkoorikute uurimisest Eestis. TPI Toimetised, 1986. Nr. 565, lk. 149-161.
About the Investigations of Reinforced Concrete Shells in Estonia.

3. Тярно Ю.А., Волтри В.Л. Некоторые вопросы экспериментального исследования железобетонных оболочек. Труды ТПИ, 1975, № 384, с. 81-87.
About the Experiments on Cement Mortar Models of Cylindrical Shells.

4. Тярно Ю.А., Круус О.В., Палу К.В. Экспериментальное исследование цилиндрических оболочек средней длины. Труды ТПИ, 1969, № 278, с. 133-142.
Investigations on Models of Cylindrical Shells.

5. Тярно Ю.А. Анализ данных экспериментального исследования моделей цилиндрических оболочек из цементного раствора. Труды ТПИ, 1988, № 669, с. 98-114.
Data Analysis of the Experimental Investigations of the Cylindrical Shell Models of Cement Mortar.

6. Тярно Ю.А. Анализ данных экспериментального исследования моделей цилиндрических оболочек из стеклопластики. Труды ТТУ, 1989, № 691, с. 117-128.
Analysis of Experimental Data of Fiberglassplastic Models of Cylindrical Shells.

7. Тярно Ю.А., Лайдра П.О., Лумэ Я.Н. Экспериментальное исследование пологих оболочек двоякой кривизны с подпертыми бортовыми элементами. Труды ТПИ, 1972, № 333, с. 57-66.
Experimental Research of Shell Roofs of Double Curvature with Supported Edge Beams.

8. Тярно Д.А., Неудорф А.Я., Ринго Т.П. Экспериментальное исследование пологих оболочек двоякой кривизны со свободными бортовыми элементами. Труды ТПИ, 1972, № 333, с. с. 67-76.

Experimental Research of Shell Roofs of Double Curvature with Free Edge Beams.

9. Тярно Д.А. Исследование пологих железобетонных оболочек ($L/l = 3$) двоякой кривизны. Труды ТПИ, 1975, № 384, с.69-80.

Experimental-Theoretical Research of Shell Roofs of Flat Double Curvature ($L/l = 3$).

10. Тярно Д.А. Анализ данных экспериментального исследования моделей трансляционных оболочек из цементного раствора. Труды ТПИ, 1985, № 569, с. 67-81.

Data Analysis of the Experimental Investigation of the Translator Shell Models of Cement Mortar.

11. Тярно Д.А. Анализ данных экспериментального исследования моделей пологих оболочек $R_1/R_2 = 10$ двоякой кривизны из цементного раствора. Труды ТПИ, 1986, № 624, с. 41-58.

Data Analysis of the Experimental Investigation of the Flat Translator $R_1/R_2 = 10$ Shell Models of Cement Mortar.

12. Тярно Д.А. Анализ данных экспериментального исследования моделей пологих оболочек $R_1/R_2 \simeq 5...10$ двоякой кривизны. Труды ТГУ, 1989, № 691, с. 105-116.

Analysis of Experimental Results of Fiberglassplastic Models of Flat Double Curvature $R_1/R_2 \simeq 5...10$ Shells.

13. Тярно Д.А. Исследование цилиндрических и квазицилиндрических оболочек с прямыми продольными предварительно напряженными стрингерами. Труды ТПИ, 1981, № 504, с. 63-77.

Investigation of Cylindrical and Quasicylindrical Shells with Straight Prestressed Cables.

14. Тярно Ю.А. Квазицилиндрические железобетонные оболочки с криволинейными бортовыми элементами. Труды ТПИ, 1983, № 551, с. 17-26.

About Quasicylindrical Reinforced Concrete Shells with Arch-like Edgebeams.

15. Тярно Ю.А. Анализ данных экспериментального исследования моделей пологих оболочек отрицательной кривизны. Труды ТПИ, 1988, № 669, с. 86-97.

Data Analysis of the Experimental Investigations of the Negative Curvature Shells.

16. Тярно Ю.А. Исследование конструкций из железобетонных трансляторных оболочек отрицательной кривизны с системами предварительно напряженных тросов. Труды ТПИ, 1980, № 488, с. 31-40.

About the Investigations of the Reinforced Concrete Negative Curvature Shells with the Systems of the Prestressed Cables.

17. Тярно Ю.А., Лаул Х.Х. О расчете цилиндрических оболочек с ребрами и отверстиями. Труды ТПИ, 1976, № 410, с. 33-42.

About Reinforced Concrete Cylindrical Shells with Ribs and Openings.

18. Тярно Ю.А. Исследование ребристых тонкостенных оболочек. Труды ТПИ, 1984, № 571, с. 43-53.

Investigations of Thin-Walled Shells with Ribs.

19. Тярно Ю.А. Исследование пологих оболочек с дискретными шарнирами с учетом поперечных нормальных сил Ту. Труды ТПИ, 1977, № 428, с. 35-40.

A Study of Flat Shells with Discrete Line Hinges by Transversal Normal Forces Ty.

20. Тярно Ю.А. Исследование цилиндрических железобетонных оболочек в стадии с трещинами. Труды ТПИ, 1978, № 443, с. 21-36.

Analysis of the Behaviour of Cylindrical Shells Crossed by Cracks.

21. Тярно Ю.А. Исследование оболочек из упругих материалов с дискретными искусственными трещинами. Труды ТПИ, 1985, № 596, с. 83–90.

Investigation on the Elastic Shells with Artificial Cracks.

22. Тярно Ю.А. О напряженном состоянии в угловых зонах цилиндрических оболочек средней длины с трещинами. Труды ТПИ, 1981, № 507, с. 63–77.

The Stress State in the Corner Zones of the Medium Length Cylindrical Shells.

23. Тярно Ю.А. Сравнение принципиальных эпюр основных внутренних сил для квазицилиндрических и цилиндрических оболочек с разными геометрическими и грузовыми параметрами. Труды ТПИ, 1978, № 443, с. 37–45.

On the Behaviour of Cylindrical and Quasicylindrical Shells with Various Geometrical and Loading Parameters.

24. Тярно Ю.А. Обобщенные схемы образования трещин в железобетонных оболочках средней длины. Труды ТПИ, 1979, № 467, с. 25–35.

About the Universal Crack Schemes for Middle Span Concrete Shells.

25. Тярно Ю.А. Применение безразмерных параметров для исследования оболочек средней длины. Труды ТПИ, 1980, № 488, с. 41–48.

Investigating Medium Length Shells by Means of Dimensionless Parameters.

Ü. Tärno

KAKSIKKÕVERATE KOORIKUTE TÖÖPRINTSIIPIDE UURIMINE MUDELITE ABIL

Kokkuvõte

Aastatel 1955 kuni 1975 tehti Eesti Teaduste Akadeemia liikme professor H. Laulu initsiatiivil, juhtimisel ja juhendamisel tema koolkonna liikmete poolt rida eksperimentaal-teoreetilisi uuringuid silindriliste raudbetoonkoorikutega. Selle laiaulatusliku töö tulemusena said võimalikuks üldistused tegelikust materjalist (peeneteraline raudbetoon) pragudega koorikute käitumise kohta. Järgnevatel aastatel uuriti tehtu täpsustamiseks erinevate kõverustega kaksikkõveraid koorikuid nii elastses kui ka pragudega staadiumis geomeetriliste parameetrite ja mõjutuste laias piirkonnas [1, 2].

Käesolevas töös on vaatluse all positiivse, null- ja negatiivse kõverusega keskmise pikkusega koorikud ääreliikmete erinevate jäikuste ja toetustingimuste puhul. Erinevate piki-, põik- ja kaldpragude ning liigendite mõju sisejõudude jaotusele uuriti elastsetel mudelitel tehispragude abil. Töös uuritud eelpingestatud elementide kasutamine võimaldab muuta sisejõudude suurusi ja jaotust konstruktorile vajalikus suunas. Sisejõudude süstematiseerimisel kasutatakse üldistuskeeme ja ühikuta parameetreid.

No 721

TALLINNA TEHNIKAÜLIKOOLI TOIMETISED
TRANSACTIONS OF TALLINN TECHNICAL UNIVERSITY

UDC 624.074

E. Gordon

ENSURING THE STRENGTH OF TALL VERTICAL CYLINDRICAL STEEL VESSELS DURING ERECTION

In constructing high-capacity plants for petrochemical, petroleum-refining and chemical industries, special attention is paid to the erection of tall vertical vessels. The latter are delivered by the manufacturer to the site fully assembled, equipped while in the horizontal position with process pipelines, servicing platforms and insulation, and then installed into their design position. The mass of such vessels may reach 1000 tons when 100 meters high.

Nowadays two basic methods of erecting tall vertical vessels are used [1], namely:

- lifting them off the ground while erecting by means of cranes or masts (see Fig. 1);
- erecting by means of cranes, rotating them around a hinge; here use is made of additional tackle devices, such as an extra pulling system or a support post with an additional polyspast (see Fig. 2).

During the lifting process in places where attaching and erection devices are connected to the vessel the wall of its cylindrical shell is subjected to considerable local loads, such as bending moments as well as radial and tangential forces. That is why one of the most important problems to be solved during design work is how to preserve the strength and to keep the shape of the vessel intact of the erection loads. That is the main factor determining reliability, safety and quality of erection work.

Attaching and erection devices are connected to the vessel shell or its skirt with the help of the following structures welded to its contour: a square sheet box, a branch pipe, and also two, four or eight twin lugs placed

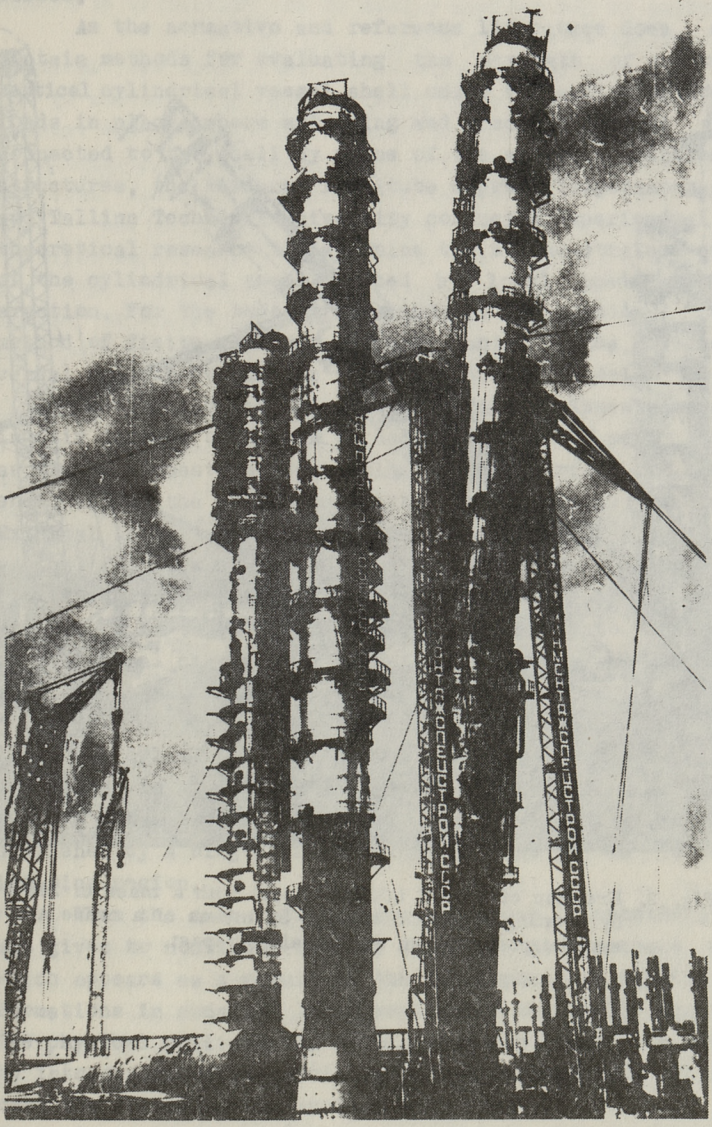

Fig. 1. Erection of a 91.4 m high vessel with a mass of 803 t by means of 1000 t capacity masts.

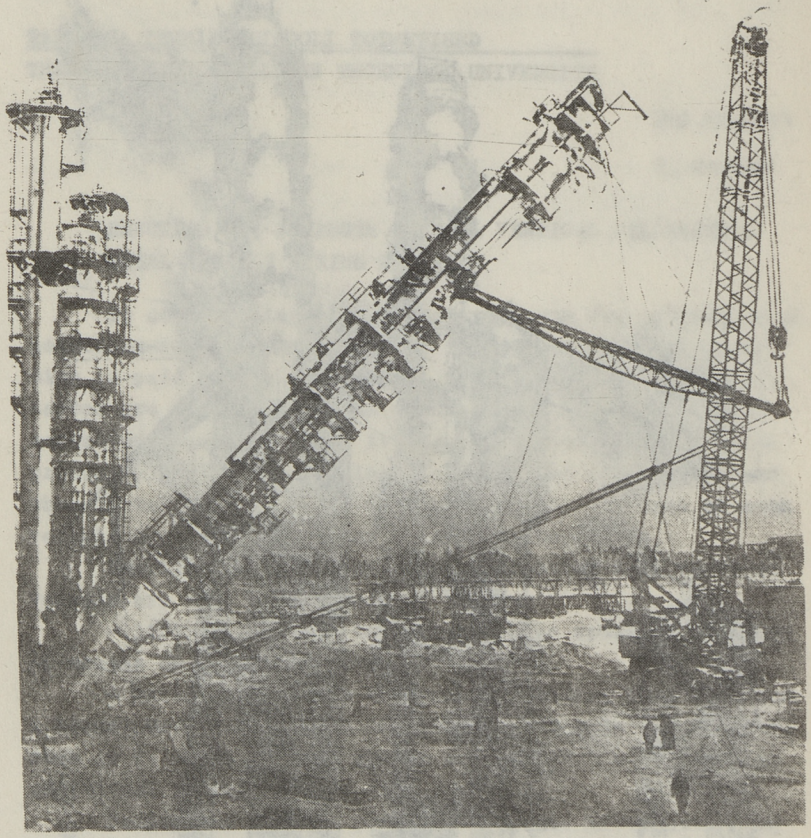

Fig. 2. Erection of a 56.3 m high vessel with a mass of 248 t by rotating it around a hinge by means of a crane and a support post with an additional polyspast.

in both the circular and longitudinal directions of the vessel.

As the normative and reference literature does not contain methods for evaluating the strength of a tall vertical cylindrical vessel shell under the action of local loads in places where attaching and erection devices are connected to the shell by means of the above mentioned structures, the Research Institute Giproneftespetsmontazh and Tallinn Technical University conducted experimental and theoretical research to determine the stress-strained state of the cylindrical shell induced by local loads during erection. For the theoretical study of the problem, the method of finite elements was used, which is the most universal one for evaluating various types of loads.

Rectangular and triangular laminated elements having six degrees of freedom in each assembly [2] were used as finite elements approximating the mid-surface of the shell and of the connecting parts for attaching devices. External load in the form of moments and radial and tangential forces was applied to the shell through the rigidly connected parts of the attaching devices. The finite element dimensions in the loading area were optimized to account for the local character of the stressed state and nonlinear work of the material.

The following two design models were used:

- a cylindrical shell freely supported at the ends and loaded in the middle of the span;

- a cantilever cylindrical shell with its free end stiffened by a ring when applying the load in the stiffening ring region.

When the calculations were performed, consideration was given to nonlinear-elastic stage of the structure work which appears as a result of the development of plastic deformations in separate local regions of the shell surface. The physical nonlinearity of the work was taken into account by introducing variable elasticity parameters [3]. In this case the following assumptions were made:

1. An idealized Prandtl diagram is valid for the structure material.

2. The variable elasticity parameters (elastic modulus

and Poisson ratio) were adopted for each finite element according to the maximum values of the "intensity of stresses" determined by formula (1).

3. The maximum permissible local load was determined for the greatest loaded point of the shell surface by limiting the development of plastic deformation. The value of the permissible intensity of deformation was determined on the basis of the experimental study and general experience of performing erection work without impairing the operational quality of the vessel shell after stress relieving. The calculations were performed in accordance with the programme "SPRINT" developed by the Department of Building Structures of the Moscow Institute of Transportation Engineers.

The theoretical calculations have revealed the clearly defined local nature of the stress-strained state of the cylindrical shell. Both the stresses and the deflections are rapidly reduced as the distance from the place of loading increases; they do not exceed 20 per cent of the maximum values at a distance of 0,6 radius of the shell.

Maximum normal stresses arise on the outer surface of the shell at the end points of contact of the shell and the connecting parts of the attaching and erection devices.

Under the joint action of local moment, radial and tangential loads, the main effect on the stress-strained state of the shell is produced by the moment and radial loads, whereas the effect of the shear forces is negligible and can be ignored during practical calculations. The stressed state is mainly characterized by bending and membrane stresses in circular and longitudinal directions. The shear stresses are relatively small, no more than 3 per cent of the maximum value. That is why the normal longitudinal (σ_x) and circumferencial (σ_y) stresses may be considered the principal ones, and the intensities of stresses at the elastic stage of the shell work may be approximated as for a two-dimensional stressed state from the following formula

$$\sigma_i = \sqrt{\sigma_x^2 + \sigma_y^2 - \sigma_x \sigma_y} \qquad (1)$$

Normal stresses σ_x and σ_y are determined by the expressions:

1. Under the action of a local moment load M

$$\left.\begin{aligned}\sigma_x &= \frac{M}{bS^2} K_1(1 + \vartheta_1) \\ \sigma_y &= \frac{M}{bS^2} K_2(1 + \vartheta_2)\end{aligned}\right\} \qquad (2)$$

2. Under the action of a radial load N

$$\left.\begin{aligned}\sigma_x &= \frac{N}{S^2} K_3(1 + \vartheta_1) \\ \sigma_y &= \frac{N}{S^2} K_4(1 + \vartheta_2)\end{aligned}\right\} \qquad (3)$$

where b - is the size of the connection unit of the attaching device and the shell in the direction of the moment action;

S - is the thickness of the shell;

K_1 to K_4 - are the coefficients depending on relative sizes of the connection unit of the attaching device and the shell and on the shell rigidity parameter $\frac{R}{S}$;

R - is the radius of the shell mid-surface;

ϑ_1 and ϑ_2 - are the relations of the membrane stresses to deflections in circular and longitudinal directions.

To check the theoretical calculations experimentally, models corresponding to the adopted designs of the connection units of the attaching devices and the vessel shell were tested. The experimental studies have corroborated the results of the theoretical calculations, highlighting the local character of the stress-strained state of the shell. Radial deflections to load relation are close to linear. After relieving the load causing deformation intensity twice the one, corresponding to the elastic limit state, practically complete restoration of deformations and deflections takes place. Comparison of the experimental and theoretical data reveals their good convergence. The maximum discrepancy does not exceed 20 per cent.

On the basis of the experimental and theoretical studies and the practical experience of performing erection work, normative documents have been developed on how to

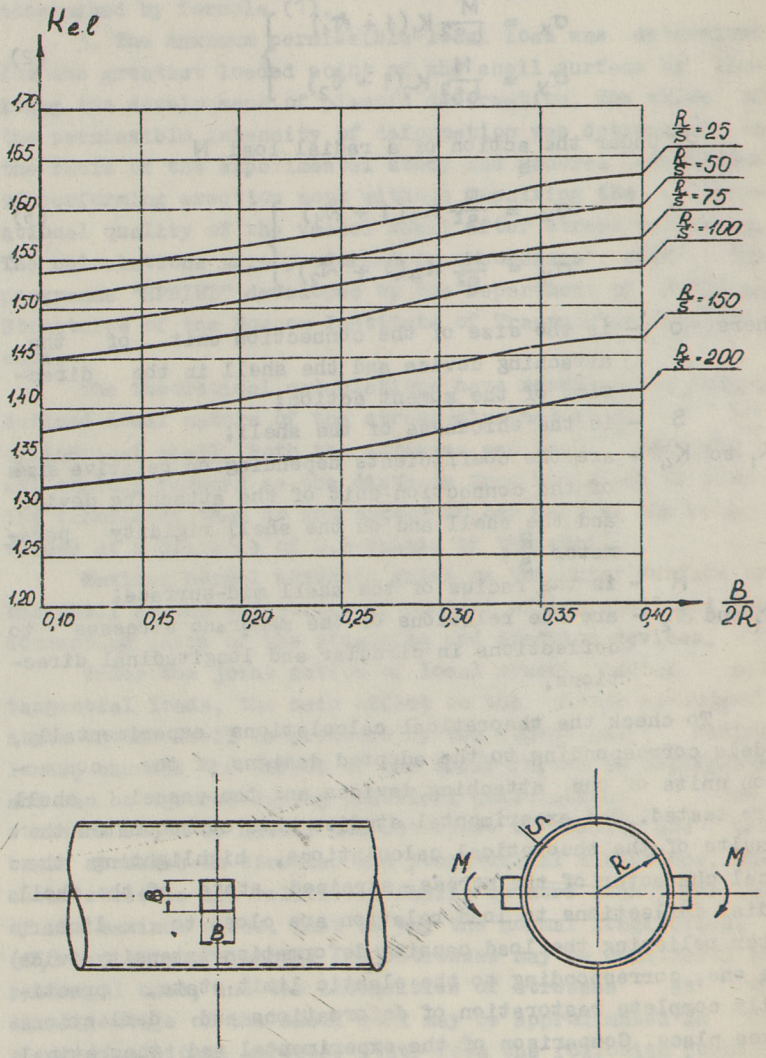

Fig. 3. Coefficient K_{el} when the circumferential moment load is applied to the vessel through a square sheet box.

ensure the strength of the skirt and the shell of a tall vertical vessel during erection [4, 5, 6].

These documents present the requirements for the design of the connection units of the attaching and erection devices and the vessel shell and its skirt; they also give the standard and design loads on the vessel during erection work as well as equations for assessing the vessel shell strength and recommendations on how to increase it.

When assigning radial and moment loads, the maximum intensity of the deformations is taken to be double the value of the intensity of the deformations corresponding to the yield limit of the structure material.

The nonlinear-elastic stage of the structure work is estimated by introducing the coefficient $K_{el} > 1$. In this case the permissible load on the vessel is calculated by the formula

$$[F] = [F]_y \cdot K_{el} \tag{4}$$

where $[F]_y$ - is the limit external load on the vessel at an elastic stage of work. It equals to

a) under the action of an external moment load

$$[M]_y = \frac{\sigma_T b S^2}{K_1(1+\bar{\alpha}_1)\sqrt{1+\left[\frac{K_2(1+\bar{\alpha}_2)}{K_1(1+\bar{\alpha}_1)}\right]^2 - \frac{K_2(1+\bar{\alpha}_2)}{K_1(1+\bar{\alpha}_1)}}} \tag{5}$$

b) under the action of an external radial load

$$[N]_y = \frac{\sigma_T S^2}{K_3(1+\bar{\alpha}_1)\sqrt{1+\left[\frac{K_4(1+\bar{\alpha}_2)}{K_3(1+\bar{\alpha}_1)}\right]^2 - \frac{K_4(1+\bar{\alpha}_2)}{K_3(1+\bar{\alpha}_1)}}} \tag{6}$$

The value of the coefficient K_{el} depends on the relative dimensions of the connection unit of the attaching device and the vessel and on the shell rigidity parameter $\frac{R}{S}$.

Values of the coefficient K_{el} are cited by way of example in Fig. 3 for the case of applying a moment

load to the shell through a square sheet box.

The above procedures can be used in design of tall vertical vessels with due consideration to their erection method.

References

1. VSN 351-88. Erection of tall vertical vessels and towers. Moscow, 1988 (in Russian).
2. Gordon E.Ya., Dubyshkina L.V. The stress-strained state of a cylindrical vessel shell in the region of the attatching rig connection. Transactions of Tallinn Polytechnical Institute, 1988, No. 669, p. 25-34 (in Russian).
3. Birger I.A. Round plates and shells of rotation. Oborongiz, Moscow, 1961, p. 265 (in Russian).
4. Calculation methods for the strength of the tall vertical vessel shell in places of fixing erection lugs and ropeless grips - RD26-02-76-88. Moscow, 1988 (in Russian).
5. Calculation methods for the strength of the tall vertical vessel shell in a place of fixing the support posts - RD26-02-78-88. Moscow, 1988 (in Russian).
6. Calculation methods for the strength of the cylindrical skirt of the tall vertical vessel in a place of fixing a hinge device - RD26-02-82-88, Moscow, 1989 (in Russian).

E. Gordon

TERASEST SILINDERREAKTORITE TUGEVUSE TAGAMINE MONTAAŽIL

Nafta- ja keemiatööstuse ehituses on eriline koht silinderreaktorite montaažil. Kasutatavate reaktorite mass võib küündida 1000 tonnini, kõrgus 100 meetrini. Reaktorite montaažil mõjuvad silinderkoorikule tõstevahendite kinnituskohal suured lokaalsed koormused painde-momentide ning radiaal- ja tangentsiaaljõudude kujul. Reaktori töö keerukuse tõttu tegid instituut "Giprotefte-spetsmontaž" ja TTÜ koostöös silinderkooriku pinge- ja deformatsioonioleku eksperimentaal-teoreetilisi uuringuid reaktori kohaliku koormamise oludes. Teoreetilisel uurimisel kasutati lõplike elementide meetodit. Osutus, et silinderkooriku pingetel ja deformatsioonidel on selgelt väljenduv lokaalne iseloom, mida kinnitasid ka eksperimentaalsed uuringud. Uurimistulemuste ja montaažitööde praktika põhjal töötati välja reaktori tugevusarvutuse metoodika montaažikoormuste mõjumisel.

Hind rbl. 1.50